U.S. ARMY, NATICK SOLDIER RESEARCH, DEVELOPMENT AND ENGINEERING CENTER
WITH THE UNIVERSITY OF CANTEBURY BIOMOLECULAR INTERACTION CENTRE

SERDP WP-1756

Identification of important process variables for fiber spinning of protein nanotubes generated from waste materials.

Research Team (listed alphabetically): Steve Arcidiacono, Megan Garvey, Juliet Gerrard, Jackie Healy, Jason Soares, Madhusudan Vasudevamurthy, Kang Wong

PI: Charlene M Mello

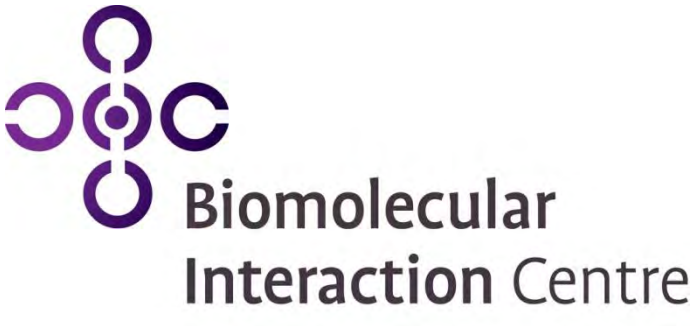

REPORT DOCUMENTATION PAGE

Form Approved
OMB No. 0704-0188

PLEASE DO NOT RETURN YOUR FORM TO THE ABOVE ORGANIZATION.

1. REPORT DATE *(DD-MM-YYYY)*	2. REPORT TYPE	3. DATES COVERED *(From - To)*
11-Jan-2012	SERDP Final Report - WP1756	FY11

4. TITLE AND SUBTITLE

Identification of Important Process Variables for Fiber Spinning of Protein Nanotubes Generated from Waste Materials

5a. CONTRACT NUMBER

5b. GRANT NUMBER

5c. PROGRAM ELEMENT NUMBER

6. AUTHOR(S)

Steve Arcidiacono, Megan Garvey, Juliet Gerrard, Jackie Healy, Jason Soares, Madhusudan Vasudevamurthy, Kang Wong

5d. PROJECT NUMBER

5e. TASK NUMBER

5f. WORK UNIT NUMBER

7. PERFORMING ORGANIZATION NAME(S) AND ADDRESS(ES)

NSRDEC, Kansas St. Natick MA 01760
University of Canterbury, Christchurch, NZ

8. PERFORMING ORGANIZATION REPORT NUMBER

9. SPONSORING/MONITORING AGENCY NAME(S) AND ADDRESS(ES)

Mr. Bruce Sartwell
Strategic Environmental Research and Development Program
Program Manager, Weapons Systems & Platforms
901 N. Stuart Street, Suite 303
Arlington, VA 22203-1853

10. SPONSOR/MONITOR'S ACRONYM(S)

SERDP

11. SPONSOR/MONITOR'S REPORT NUMBER(S)

WP-1756

12. DISTRIBUTION/AVAILABILITY STATEMENT

UNLIMITED

13. SUPPLEMENTARY NOTES

Final Report approved by sponsor for publication online.

14. ABSTRACT

A. BACKGROUND: Current composites for the military (e.g. carbon fibers) are typically derived from polyacrylonitrile (PAN) polymer fibers. Synthesis utilizes toxic chemicals, volatile organic solvents and extremely high temperatures. The technical approach herein addresses these shortcomings by replacing said toxic materials with protein nanotubes/nanofibrils generated from waste materials and utilizing aqueous based fiber spinning to eliminate the need for hazardous processes.
B. OBJECTIVE: This effort brings together the expertise of Professor Gerrard's team at the University of Canterbury, New Zealand with that of the U.S. Army Natick Soldier Research, Development and Engineering Center (NSRDEC) for the development and characterization of military relevant fibers. We have specifically explored the feasibility of spinning protein nanotubes into fibers and initiated characterization of the properties of such fibers. Our deliverable includes methods for controlling nanofibril structure, spinning fish lens protein into fibers, identification of important spin dope processing and fiber spinning parameters for further opti

15. SUBJECT TERMS

Fibers, biopolymer, sustainable materials, protein based materials.

16. SECURITY CLASSIFICATION OF:			17. LIMITATION OF ABSTRACT	18. NUMBER OF PAGES	19a. NAME OF RESPONSIBLE PERSON
a. REPORT	b. ABSTRACT	c. THIS PAGE			Charlene Mello
Unclass	Unclass	Unclass	Unclass	49	19b. TELEPHONE NUMBER *(Include area code)* 508-990-9679

Reset

Standard Form 298 (Rev. 8/98)
Prescribed by ANSI Std. Z39.18

CONTENTS

LIST OF FIGURES

LIST OF TABLES

LIST OF ACRONYMS

BCA	Bicinchoninic Acid (protein assay)
CC10	Centricon 10
DTRA	Defense Threat Reduction Agency
DTT	Dithiothreitol
EDTA	Ethylenediaminetetraacetic acidFLH Fish lens homogenate (crude crystallin preparation)
HAP	Hazardous air pollutant
HCl	Hydrochloric acid
HPLC	High-performance liquid chromatography
IPA	isopropanol
MC10	Microcon 10
MeOH	Methanol
MES	2-[N-morpholino]ethanesulfonic acid
MWCO	Molecular weight cut off
NSRDEC	Natick Soldier Research, Development & Engineering Center
PAN	Polyacrylonitrile
PEEK	Polyether ether ketone
POM	Polarized optical microscopy
PT	Phosphate-Tris (spinning buffer)
SDS-PAGE	Sodium dodecyl sulfate polyacrylamide gel electrophoresis
SEM	Scanning electron microscopy
TEM	Transmission electron microscopy
TFE	Trifluoroethanol
TMV	Tobacco mosaic virus
XRD	X-ray diffraction
USDA	United States Dairy Association

KEYWORDS

Aqueous based fiber spinning
Sustainable technology
Crystallin proteins
Nanofibril spinning

ACKNOWLEDGEMENTS

We are grateful to Dr. John Walker for his insightful discussions and recommendations. Ms. Elizabeth Welch, Mr. Joseph Senecal and Mr Animesh Agrawal are thanked for their assistance with fiber spinning and microscopy. Financial support from Bruce Sartwell , Weapons Systems & Platform Program Manager for the Strategic Environmental Research and Development Program (SERDP) is is greatly appreciated.

ABSTRACT

A. BACKGROUND: Current composites for the military (e.g. carbon fibers) are typically derived from polyacrylonitrile (PAN) polymer fibers. Synthesis utilizes toxic chemicals, volatile organic solvents and extremely high temperatures. The technical approach herein addresses these shortcomings by replacing said toxic materials with protein nanotubes/nanofibrils generated from waste materials and utilizing aqueous based fiber spinning to eliminate the need for hazardous processes.

B. OBJECTIVE: This effort brings together the expertise of Professor Gerrard's team at the University of Canterbury, New Zealand with that of the U.S. Army Natick Soldier Research, Development and Engineering Center (NSRDEC) for the development and characterization of military relevant fibers. We have specifically explored the feasibility of spinning protein nanotubes into fibers and initiated characterization of the properties of such fibers. Our deliverable includes methods for controlling nanofibril structure, spinning fish lens protein into fibers, identification of important spin dope processing and fiber spinning parameters for further optimization as well as a qualitative comparison of the properties of the fibers for selected variables explored.

C. SUMMARY OF PROCESS/TECHNOLOGY: Prof. Gerrard leads two research programs in NZ, centered on the generation of protein nanotubes from waste materials for use in various bionanotechnologies. Inspired by the synthesis routes and properties of natural fibers, the research team at the U.S. Army NSRDEC has used liquid crystalline solutions of structural proteins[1-5] and rod-shaped bacterial viruses[6] as precursors to fabricate functional fibers. This Limited Scope effort has enabled us to merge these existing capabilities and explore the feasibility of preparing military relevant fibers from renewable waste protein materials (e.g. eye lenses proteins). A systematic evaluation of aqueous based wet-spin processing parameters necessary for the generation of protein based fibers has been conducted. Characterization of molecular alignment was conducted using optical microscopy and qualitative properties of the fibers have been determined. In addition, conditions were defined for the control of nanofibril structure enabling the formation of extended nanofibrils (to several microns), highly branched nanofibril networks, or bundled nanofibrils. A recommendation for future research centered on the feasibility of replacing nylon fibers with these environmentally friendly materials is presented.

D. BENEFITS: The availability of fibers that can be spun or assembled at high concentrations from sustainable resources and environmentally friendly processes, and in which the fibers themselves have structural integrity provide the potential for multi-functionality. A broad range of military relevant applications are possible such as higher-strength bioplastics and nanocomposites, water-repelling coatings, textiles, immobilized catalysts, surface-active packaging, enzyme reactors, decontamination of chemical and biological warfare agents, bioremediation, and even electronics.

E. TRANSITION PLAN: The knowledge obtained through this effort has been communicated through technical presentations at the SERDP Partnership Conference and other venues. Successful generation of protein nanotube based fibers and the observed properties of these materials have resulted in a clearer definition of specific application areas. Appendix IV provides a letter of interest from Dr. John LaScala, ARL. We aim to explore the feasibility of replacing nylon based materials at the NSRDEC Fiber Center of Excellence in a follow-on effort with SERDP.

OBJECTIVE

Biology offers several advantages over traditional systems for the construction of novel materials. These include self-assembly, exploitation of molecular diversity, sustainability, environmentally friendly processing conditions, and new synthesis routes to manufacturing multifunctional fibers. Current petroleum-based polymers and fibers are typically derived using hazardous processes and toxic materials. We have addressed both of these shortcomings by replacing said toxic materials with protein nanotubes generated from waste materials and utilizing aqueous based fiber spinning to eliminate the need for hazardous processes. This effort brings together the expertise of Professor Gerrard's team at the University of Canterbury, New Zealand with that of the NSRDEC for the development and characterization of military relevant fibers. A systematic evaluation of the processing parameters necessary for the generation of nanotube based fibers has been conducted. Characterization of fiber properties was also investigated to identify the most important processing conditions for optimization, further research and development.

BACKGROUND

Definition of the problem: Current composites for the military are often made from fibers derived from petrochemical feedstocks. For example, carbon fibers are routinely derived from specialized PAN fibers. PAN fibers used in production of carbon fibers are different than the more commonly recognized PAN fibers used in the textile industry. Often they vary with respect to chemical compositions, type and amount of co-monomers, cross sectional area, linear density and tensile strength. At present, PAN fibers are composed of at least 85% by weight acrylonitrile; while the remaining 15% consists of neutral and/or ionic co-monomers. Neutral co-monomers such as methyl acrylate, vinyl acetate, or methyl methacrylate are used to adjust the solubility of the acrylic copolymers in spinning solvents and control the acrylic fiber morphology. Ionic and acidic co-monomers such as those containing sulfonate groups and itaconic acid provide dye sites and increase hydrophilicity [7].

Manufacturing carbon fibers from these PAN-based precursors entails a two step process including stabilization and carbonization. Prior to stabilization the fibers are heated to approximately 180 to 300^{o}C in an oxygen-containing atmosphere to improve orientation and crosslink the molecules. The chemistry of stabilization is complex, but primarily consists of cyclization of the nitrile groups, dehydrogenation and oxidation. Non-carbon elements are removed through the second step of carbonization which involves heat treatment of the stabilized PAN fibers. Such elements are displaced in the form of a gas such as water, ammonia, carbon monoxide, hydrogen cyanide, carbon dioxide and nitrogen. Carbonization is carried out at temperatures ranging from 1000 to 1500^{o}C in an inert atmosphere [8-10].

Highly crystalline and oriented ultrahigh-molecular-weight polyethylene fibers also have excellent potential for composite materials because of their high strength and low density. As a result, these materials are being considered for future composite applications in the military, including vehicle armor and aircraft. Overall, the regular molecular and/or crystalline structure enables them to have superior performance relative to other fibers. Therefore, highly purified bio

products would most likely be required in order to produce highly regular molecular/crystalline structures to enable the formation of high performance fibers. The lens crystallin protein source selected for these studies can be collected in a very pure form and is an abundant source of waste material. In addition, a processing method must be determined to produce highly oriented fibers from the bio-based materials. This processing method should be environmentally friendly and use no toxic or hazardous air pollutant (HAP) solvents. As will be described in detail below, the NSRDEC has previously demonstrated the feasibility of processing biological materials (silk and nanotube like bacteriophage) into highly oriented fibers with an aqueous based wet-spinning process. Building upon this expertise, we describe in the results section details of processing and spinning crystallin lens proteins.

Our preliminary data and experimental approach address many of the technical hurdles necessary for the implementation of composite materials generated from renewable resources. Processing of these protein based nanotubes into fibers is conducted in an aqueous environment at ambient temperature. Furthermore, this process has the potential to be a cradle to grave renewable, sustainable, and environmentally friendly method with very low energy demands and derived from non-food sources.

Natural fibers: Natural fiber composites have garnered interest in the composite industry as an alternative to synthetic polymer composites. Vegetable or plant-based natural fibers including flax, hemp, cotton, sisal, and kenaf[11] and animal-based natural fibers including wool, hair and silkworm silk alleviate environmental concerns associated with production of synthetic materials. The natural fibers possess high stiffness, non-brittle fracture behavior, are generated from cost-effective, renewable resources and are biodegradable, generally being isolated through mechanical approaches and being incorporated into commodity thermoplastics [12,13]. However, the benefits of the environmentally friendly natural fibers are minimized when used with polymer matrices such as polystyrene or polypropylene, which are non-biodegradable and petroleum-based. This has lead to the development of biocomposites comprising natural fibers and biodegradable, renewable polymers such as cellulosic plastics, soy-based plastics, and polyhydroxyalkanoates [14,15]. Unfortunately, several constraints have limited their more widespread incorporation into products including thermal stability, moisture absorptivity, and impact strength.

Aqueous based fiber spinning

Spider Silk: The first fiber in the world was made by nature and in fact nature has produced the strongest fiber. These are spun from the spinnerets on a spider's abdomen. The spider extrudes pure liquid silk protein from these spinnerets and uses their legs to draw the fibers, thereby improving molecular alignment and increasing fiber strength. The structural fibers of the golden orb-weaver spider *Nephila clavipes* have been most extensively studied [2-3, 16, 17]. Like most spider silks, they are extremely strong and flexible, absorbing impact energy from flying insects without breaking. Dragline silk fibers dissipate energy over a broad area and balance stiffness, strength and extensibility. These fibers are three times tougher than aramid fibers and five times stronger by weight than steel. Therefore, spider silk fibers possess the desirable mechanical properties for lightweight, high-performance fiber, and composite applications.

Spiders produce these materials from an aqueous solution under ambient temperature and pressure, in contrast to hazardous solvents and harsh conditions needed to produce synthetic fibers. The dragline fiber is predominantly proteineacous, comprised of greater than 80% glycine, alanine, and other short side chain amino acids [16] with crystalline regions of anti-parallel β-pleated sheets [17]. Furthermore, the molecular orientation within the dragline fiber is optically evident by birefringence. Inspired by the synthesis and properties of natural fibers, the NSRDEC team was the first to report and patent technologies for spinning recombinant silk fibers with an aqueous based, environmentally friendly process [1-3]. Briefly, purified silk solutions were concentrated using a multi-stage ultrafiltration approach. A specially designed spinneret was developed to mimic the spider's spinning process from the gland. This spinneret oriented the silk molecules in the spin solution, causing self-assembly and induction of fiber formation. Individual fibers were 10-60 μm in diameter, water insoluble, and exhibited molecular orientation as revealed by birefringence (Figure 1).

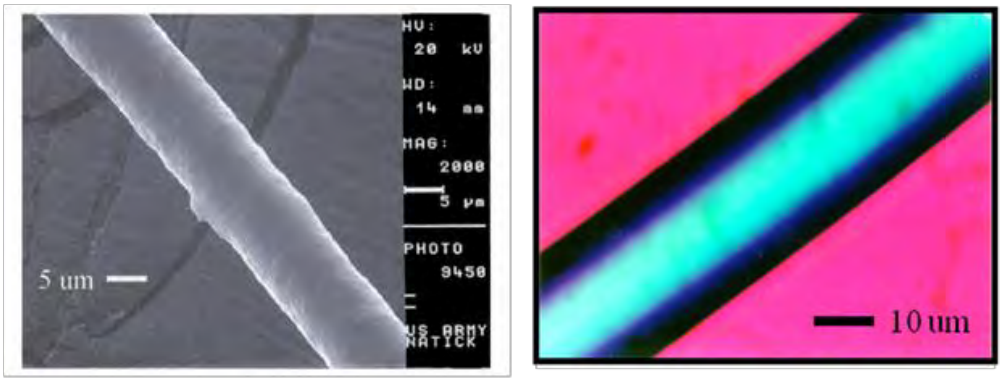

Figure 1. A) Scanning electron micrograph of a $[(SPI)_4/(SpII)_1]_4$ fiber spun from a 21.5% spin solution. The fiber was drawn to 2.5 its original length. B) Birefringence of a recombinant spider silk fiber produced by an aqueous spinning process under polarizing light (first-order 530 nm red plate) reveals molecular alignment/orientation.

Mechanical properties were influenced at least in part by several variables: protein concentration and purity, coagulation bath composition, and post-spin draw. A silk protein concentration of 10% or more was required for fiber formation while solutions of >70% purity were required to minimize fiber brittleness. Coagulation bath composition was optimal from 70-90% methanol (MeOH) in water. Post-spinning draw imparted molecular orientation needed for improved mechanical properties. Mechanical integrity of the fibers improved as draw increased. The fiber could be drawn up to five times its original length in a single and deliberate motion to enhance the toughness of the single fibers from ~0 MPa to 47 MPa. Implementation of a double draw technique by which a single twofold draw in the coagulation bath followed immediately by a threefold draw in 100% water resulted in further enhancement of the toughness to 71 MPa. Unfortunately, spiders are not capable of producing the quantities of silk necessary for fiber spinning studies. To address this problem recombinant spider silks have been expressed by our team members and others [16, 17] producing sufficient quantity for the laboratory scale fiber spinning experiments summarized above. To date, scaling the production of spider silk to a quantity necessary for commercialization has been unsuccessful despite attempts by numerous groups (many of whom have had active collaborations with our group).

Rod-shaped viruses: Among all biological materials, viruses and viral like particles have recently attracted much attention for the development of novel biocomposite materials. Rod-like biomacromolecular assemblies, such as M13 bacteriophage and tobacco mosaic virus (TMV), have well-defined structural features, high aspect ratio, narrow size distribution, and good water solubility [18-30]. Bacteriophage are very stable and can endure treatment within a wide range of pH, solvents and temperatures. Moreover, the surface functionalities and properties of these bionanorods can be easily manipulated either by traditional bioconjugation methods or genetic engineering without disrupting their integrity [19-23, 27, 30]. Due to these properties, TMV and M13 are particularly interesting scaffolds for developing multifunctional fiber based materials [6, 19, 22, 23, 26, 30].

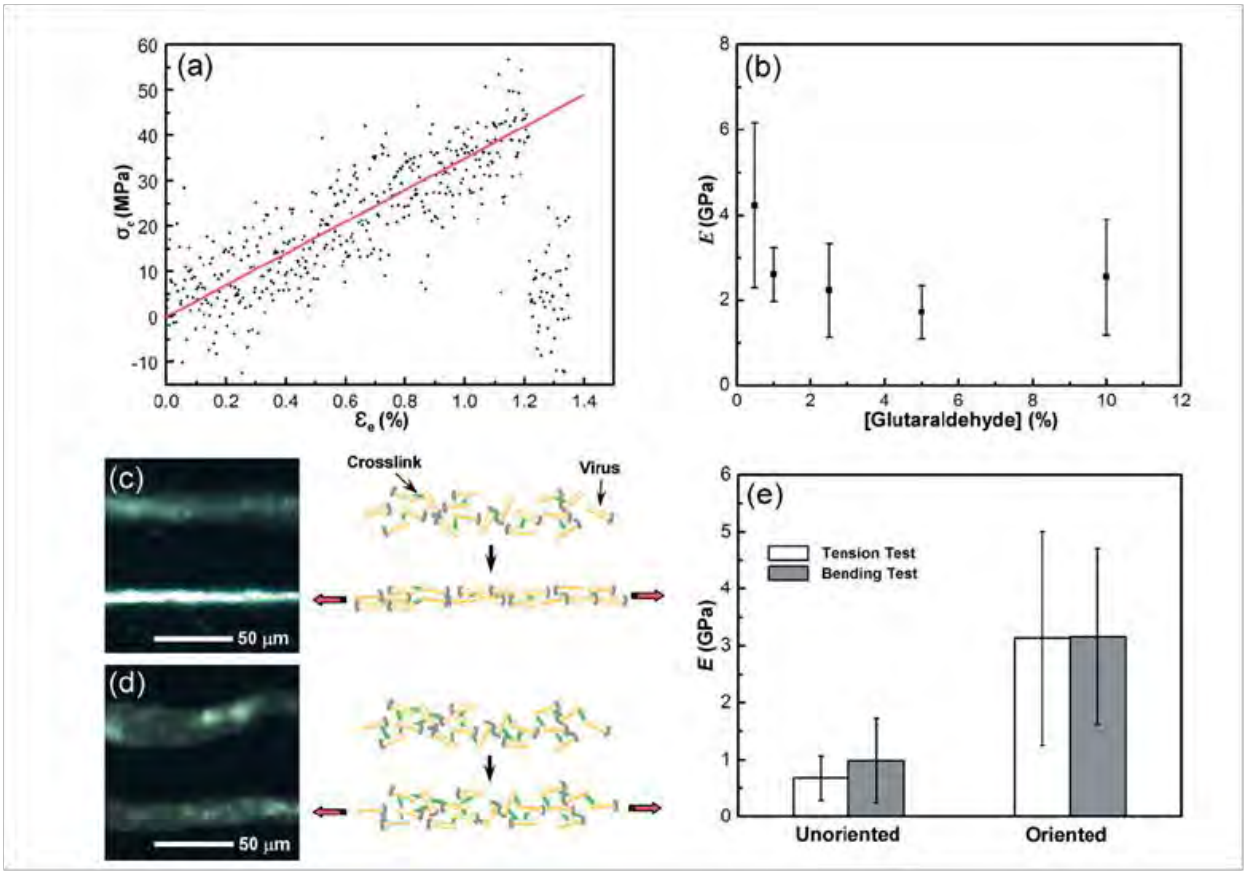

Figure 2. Mechanical properties of virus fibers. a) Representative engineering stress–strain response of virus fibers. No plastic deformation is observed until fiber fracture. b) Effects of glutaraldehyde concentration on the Young's modulus *E* shows a local minimum around 5% glutaraldehyde. c,d) Polarized optical microscopy (POM) images of virus fibers (left) and schematic graphs of virus assemblies (right), where rods represent individual virus particles constrained by crosslinks (green). The virus fibers fabricated from 0.5% (c) and 5% (d) glutaraldehyde solutions before stretching (top) and after manual elongation while drying (bottom). e) Comparison of *E* for unoriented and oriented virus fibers consisting of 0.5% glutaraldehyde solution under uniaxial tension test and cantilevered bending test.

In previously published work, we have demonstrated the capability of M13 bacteriophage to be used as the raw material for functional fiber formation [6, 30]. As proof of principle, we utilized a genetically designed gold-binding M13 filamentous virus and demonstrated the capability of M13 bacteriophage to retain this specific surface functionality when spun into a functional fiber. Again, a wet-spinning process was utilized; the concentrated virus solution (~470 mg/ml) was spun into 2.5% (v/v) glutaraldehyde solution [6]. All fibers could be pulled out of the solution by using forceps, indicating sufficient strength for mechanical processing such as drawing and weaving. Uniaxial tensile tests were conducted to examine the mechanical properties of these virus fibers in the dry state (Figure 2a). On average, engineering stress–strain responses of pure virus fibers indicated a Young's elastic modulus E of ca. 3 GPa, an ultimate tensile strength σ_u of ca. 33 MPa, and an ultimate tensile strain ε_u of ca. 1.3 %. Overall, E of the pure-virus fiber was similar to that of Nylon 6,6 (E= 1–3 GPa) and glassy homopolymers such as polystyrene (E= 2–4 GPa). Fiber ultimate tensile strength σ_u was comparable to that of atactic polystyrene and polytetrafluorethylene (σ_u = 15–50 MPa).

The effects of Young's modulus (Figure 2b) and virus orientation on fiber crystallinity were observed using tensile testing and polarized optical microscopy respectively (Figure 2c-d). The crystallinity of the virus fibers with low cross-linking density can be easily increased by drawing the wet fibers. This elongation process reorients the virus particles and promotes secondary interactions among viruses. In addition, an independent set of samples was tested under uniaxial tension and bending to examine the effects of virus orientation on fiber mechanical properties (Figure 2e). In this experiment, oriented fibers were elongated at least 15% in the wet state and analyzed to measure E in the dry state. Under uniaxial tension, the stiffness E of the oriented virus fiber (3.13 ± 1.88 GPa) increased significantly compared to the unoriented fiber (0.68 ± 0.39 GPa) and that the strength σ_u of the oriented fiber (35.05 ± 25.53 MPa) also increased significantly with respect to the unoriented counterpart (6.02 ± 5.40 MPa). It was therefore concluded that the crosslinker is only needed to process the virus fibers via spinning but is not necessary to enhance the mechanical with that measured via uniaxial tension. In the case of virus fibers with low chemical crosslinking densities, both the mechanical strength and stiffness is attributable to secondary interviral interactions such as hydrogen-bonding and ionic interactions, and the mechanical properties can be enhanced through fiber elongation that promotes crystallinity via environmentally benign processing.

Alternative source of protein: Although spinning of spider silk and bacterial viruses have proved successful, the need for an alternative protein source that is abundant, pure and inexpensive remains. Professor Gerrard's group at the University of Canterbury, New Zealand is producing very promising candidates to meet this need. They have developed an approach to self-assemble protein nanotubes from a range of pure, semi-purified and crude protein sources, currently all New Zealand-sourced protein waste materials. New Zealand has a surfeit of protein that could be used for the production of protein nanotubes. For example, the research team has calculated that a single cattle eyeball provides approximately 5 g of useable protein extract for the production of protein nanotubes. In 2006, 2.3 million cattle were slaughtered in NZ, providing 11.7 tons of protein for nanotube manufacture. If all of the 11.7 tons of available bovine eye lens protein was converted into high value protein nanotubes, which sold at the same current cost as carbon nanotubes, this would equate to a $788 million industry. In the USA, the potential to source eye lenses from cattle is obviously much larger: according to the United

States Dairy Association (USDA) web site, over 30 million cattle are slaughtered each year, providing over 150 tons of starting material that would otherwise go to waste. Other readily available sources of waste protein include fish eye lenses and wheat proteins.

Protein Nanotubes: These nanotube structures have a range of interesting features that make them attractive for nanotechnological applications, for example they are capable of self-assembly, well-ordered and incredibly stable, comparable in strength to steel, enzyme (protease) resistant, have variable and potentially tailorable structural features (length and morphologies), and have potential advantages over carbon nanotubes due to the ability to functionalized them [31]. The nanotubes are a highly ordered, insoluble form of protein. Fibrils are defined by a number of characteristics including an elongated, unbranched morphology, the ability to bind dyes such as Congo red and thioflavin T. One of the benefits of protein nanotubes is their ability to self assemble, which provides an attractive feature for material manufacturers [32-34]. This association is a result of non-covalent interactions, rather than covalent bonds [33], which introduces a level of control via ready manipulation of fibril formation conditions through pH and temperature variation and chemical modification [31, 32]. In addition, there is a readily available and inexpensive source of protein. Numerous studies have demonstrated the conversion of a normally soluble protein into fibrils, by subjecting the proteins to mildly destabilizing conditions that allow the proteins to partially unfold and then refold to form fibril structures. Professor Gerrard's contribution has been to adapt these methods to heterogeneous sources that are readily and cheaply available (program funded by the New Zealand Government, "Protein nanotubes for bionanotechnologies", $2.49 million over 5 years) and to develop methods to functionalize these components (Defense Threat Reduction Agency (DTRA)-funded program, "Self-assembling protein nanostructures – incorporating active functionality"). They have demonstrated the ability to scale up production of protein nanofibrils within the auspices of this Limited Scope effort. Gram quantities of fibrils in a variety of morphological forms are now possible. Details of this work are presented in Appendix II. Furthermore, NSRDEC has demonstrated the ability to spin these proteins into fibers with an average diameter of 35μm. Details of this accomplishment are provided in the results section.

MATERIALS & METHODS

Isolation of crude crystallin proteins

A supplier and source for the acquisition of waste protein has been identified enabling numerous preparations of protein nanotubes conducted from the lens of *Melanogrammus aeglefinus* (haddock). This is an abundant source with widespread availability throughout our geographical area and can be acquired on a daily basis if necessary yielding large quantities of crystallin protein for fiber spinning. Homogenization was optimized to produce samples of high protein concentration. Typical fish lens homogenate (FLH) are prepared as follows: fresh fish heads were obtained from the local fish market and the lenses were immediately extracted, cleaned and either homogenized or frozen for future use. For extraction of crystallin proteins, the lens were thawed or homogenized with the extraction buffer (50 mM Tris, 5 mM Ethylenediaminetetraacetic acid (EDTA) and 1 mM Dithiothreitol (DTT), pH 7.5). FLH solutions were aliquoted and stored at -20^{o}C.

FLH processing for Aqueous Fiber Spinning

FLH was thawed on ice for 3-4 hrs and clarified by centrifugation at 16000 g for 30 minutes at 4^{o}C. Supernatant was removed (opaque in color) and transferred to 3500 MWCO SpectraPor 3 dialysis tubing (prepared according to manufacturer's instructions) and placed in a beaker containing dialysis buffer (also termed spin buffer). For dialysis under denaturing conditions, the buffer consisted of 160 mM urea, 10 mM NaH_2PO_4, 1 mM Tris-HCl supplemented with 0-100 mM glycine pH 5.0. For non-denaturing conditions, a buffer consisting of 10 mM NaH_2PO_4, 1 mM Tris-HCl supplemented with 0-100 mM glycine or 0.2-0.6 mM L-arginine or 0.2 mM L-lysine-HCl was utilized. Typically, dialysis buffer containing glycine was adjusted to pH 5.0, but spin buffer containing arginine and lysine were utilized without pH adjustment, resulting in final buffer pH of 10.4-10.6 and 5.2 respectively. Dialysis consisted 50x volume changes at 1 hr, 2 hr and overnight respectively. Samples were gently stirred at 4^{o}C during buffer exchange. Samples were removed and centrifuged at 16000 g for 30 minutes at 4^{o}C. Supernatant was collected and transferred to Centricon 10 (CC10) ultrafiltration system (Millipore Corp) for sample concentration through a 10000 MWCO membrane at 5000 g for 30 min intervals at 4^{o}C. After each interval, the filtration unit was gently tapped to mix. Typical target volume reduction is 2.5-fold after 2 hrs but the actual reduction varied between 2-4 fold depending on the spin buffer composition. After a target volume was reached, the retentate was collected by inversion and clarified by centrifugation at 16000 g for 30 min at 4^{o}C. CC10 retentates were stored at 4^{o}C. In the case of samples containing glycine, the liquid phase was collected and transferred to a Microcon 10 (MC10) ultrafiltration system (Millipore Corp) for further volume reduction at 5000 g for 30 min intervals at 4^{o}C. Target final volume is ~50 µl. The MC10 retentate is collected by inversion and clarified by centrifugation at 16000 g for 30 min, 4^{o}C. Supernatant is collected and stored at 4^{o}C. At each stage of the processing procedure, aliquots were taken for quantitation via a microplate-based Bicinchoninic Acid Assay (BCA, prepared according to manufacturer's instructions, Pierce, Inc.) using bovine serum albumin as the standard.

Gel electrophoresis: SDS-polyacrylamide gel electrophoresis (SDS-PAGE) analysis was performed on all fractions collected throughout the processing procedure using 4-12% NuPAGE Bis-Tris gels (prepared according to manufacturer's instructions, Invitrogen Inc.) with MES as the running buffer. The resulting gels were stained with Coomassie Brilliant Blue and destained in 10% MeOH, 7.5% acetic acid. Gel images were captured using a Nikon D1 digital camera.

Evaluation of coagulation and cross-linking agents for fiber spinning

To evaluate coagulation properties of spin dopes (i.e. concentrated retentates), coagulation tests were conducted using a 100 µl Hamilton syringe. The syringe has a similar diameter to that of the spinneret used during spin trials (diameter = 0.006"). The vial used for the coagulation test is chosen to mimic the distance of the spinneret to the bottom of the coagulation bath seen within a spin trial. This enables more accurate translation of coagulation test to spin trials. The coagulation buffers used during these tests were: 40%, 50% and 60% isopropanol (IPA) and 40%, 50% and 60% MeOH. Sample (~10 µl) was dispensed into the coagulation buffer manually. Variables that were recorded include time to coagulation, distance to coagulation, fiber durability after coagulation and fiber color. Coagulation bath for spin trial is determined by

the coagulation test conditions that result in fiber formation ½ down the vial, display a dull white color after 1-2 minutes of coagulation and remain intact with gentle agitation.

Fiber spinning

Fibers were spun into a coagulation bath determined through coagulation test described above. For spin dopes containing glycine or arginine, typical coagulation bath consisted of 50% MeOH/water or 60% IPA/water respectively. Fibers were spun using a Harvard Apparatus Infusion/Withdrawal pump (Harvard Apparatus) with a specialized microspinner (cavity volume 0.5 mL, 5 mm i.d.), and 0.006 or 0.010 in I.D. Polyether ether ketone (PEEK) High-performance liquid chromatography (HPLC) tubing (Sigma-Aldrich). Typical spin dope volume was 50 µl although up to 75 µl was spun into fibers. Spin solutions were extruded into the coagulation bath at a rate of 2-10 µl /min. As-spun, undrawn fibers were collected by hand from the coagulation bath using flat nosed tweezers and submersed into a room temperature water bath. Drawn fibers were manipulated by hand and stretched unilaterally (holding one end stationary and pulling the other) 1.5-2.5x its original length (termed fold draw) within the coagulation bath. Drawn fibers were removed from the coagulation bath by tweezers and held constrained upon submersion into a water bath. Fibers were removed from the water bath after 1-2 minutes and allowed to dry either constrained or unconstrained prior to placing in a plastic petri dish. Fibers were stored in a box at ambient temperature and 60% relative humidity.

Microscopy

Fiber diameter and appearance were determined by using an Optiphot2-pol polarizing microscope (Nikon Inc.). Images were captured under both common white light and birefringence using a Nikon D1 digital camera. Under common white light, visual defects including breaks, pits, bends and cracks and diameter thinning along the fiber were recorded. Under polarizing light, birefringence, which is used to evaluate molecular alignment of the biopolymer chains along a fiber, was observed using a 530 nm first-order red plate, in some cases. Under birefringent conditions, a blue color is indicative of molecular alignment while a lack of color indicates less than optimal polymer chain alignment. For Scanning Electron Microscopy (SEM) analysis, fibers were coated with gold/palladium and viewed on a CSM 950 SEM (Carl Zeiss, Jena, Germany) at 20 keV.

Mechanical Testing

Fibers a minimum of 1.5” in length (1/2" gauge length for testing) with minimal defects within the testing area, as pre-determined by microscopy, were selected for mechanical analysis. For fibers selected for testing, denier determination was performed by conversion of an average diameter (minimum of five readings along the length of a fiber) determined through microscopic evaluations. Mechanical testing was performed using the Instron Model 55R4201 (Instron Corporation, Canton MA) at 23°C and 50% relative humidity. A 250 gram load cell with pneumatic pinch grips were utilized at a crosshead speed of 127 mm/min and a sample rate of 100 pts/sec. Single fibers were manually loaded into the grips with pneumatic closure via an air valve foot pedal using 50 psig nitrogen. Mechanical properties were calculated using the Instron software Blue Hill II.

RESULTS & DISCUSSION

Broad Survey of Variables and Approaches for Rapid down selection

The original proposal presented two very different fiber spinning approaches based upon our previously published methods 1-3. Strategies for spinning from soluble protein homogenates and nanofiber preparations were initially evaluated in parallel. Protein nanofibers were prepared from soluble crystallin proteins using published methods that have subsequently been optimized in this program for scaled up preparations (gram quantities). In addition, variables were explored and identified to control nanofibril length, degree of branching and bundling to improve molecular entanglements and macroscopic assembly features (data presented in appendix II).

A multivariate approach was utilized for the identification of important processing and spinning variables including soluble protein or nanofiber concentration, buffer compositions, nanofiber morphology (length, degree of branching and bundling), coagulation or crosslinking bath composition, spins speed, spinneret dimensions, fiber draw ratio and temperature. Although there are unique advantages to the two proposed spinning approaches, to ensure successful completion of the stated objectives of the Limited Scope effort, it was necessary to rapidly select and focus on a single approach. Conditions which yielded fibers with sufficient mechanical integrity to withstand removal from a coagulation bath were selected and investigated systematically for the remainder of the program. Such conditions were defined as soluble fish lens homogenate spun into a coagulation bath in the absence of cross linker. A summary of these investigations are presented herein. Additional data associated with control of nanofibril morphology, cross linking of soluble protein preparations and fiber spinning into a cross linking bath are presented in the appendices. Appendix I provides a synopsis of preliminary experiments to determine a suitable combination of protein/nanofiber concentration and coagulation/cross-linking bath composition. Determination of processing conditions to tailor and control nanofibril length, branching and bundling are presented in Appendix II. A detailed analysis of fibers created during spin trials described below is presented in Appendix III. The tables consist of the solution, spinning and post-spinning conditions in which the fibers were formed and also the microscopic information acquired for each fiber. Appendix IV includes a letter of interest from Dr. John La Scala, Army Research Labs.

Production and characterization of soluble protein spinning solutions

An abundant source of waste protein material has been identified at a local fish market (Captain Franks, New Bedford Massachusetts). Haddock (*Melanogrammus aeglefinus)* lenses can be acquired on a daily basis if necessary and yield large quantities of crystallin protein for nanofibril formation and fiber spinning. During the first quarter of this effort, Dr. Megan Garvey (from the lab of Prof Juliet Gerard, University of Canterbury Christchurch, New Zealand) spent four weeks in our lab sharing methods for eye lens

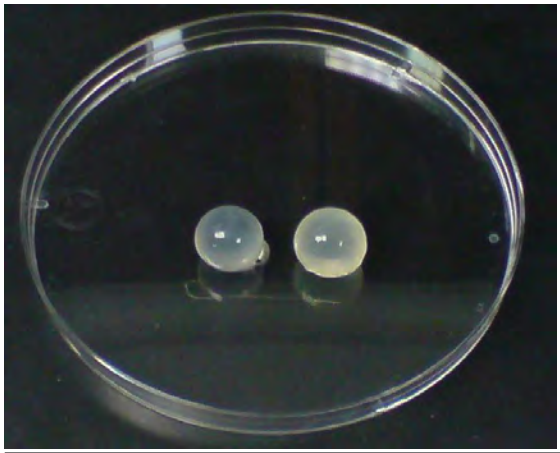

Figure 3: Haddock eye lenses which are utilized for crystalline protein preparations, nanofibril generation and fiber spinning.

dissections (see Figure 3), crystallin protein preparations (i.e. FLH), and nanofibril formation. Since this time, we have extracted numerous batches of protein, evaluated the impact of processing condition on nanofibril structure, conducted coagulation studies of FLH, spun fibers from concentrated FLH preparations and initiated characterization of these fibers.

In the initial studies, FLH solutions had a significant amount of insoluble material due to amorphous aggregation. It was difficult to remove these aggregates and therefore yielded a suspension not a solution. To achieve fibers with sufficient integrity for manipulation (i.e. drawing, collecting, etc.) and subsequent characterizations (i.e. microscopic analysis and mechanical testing), the spin dope must be free of suspended particles as they are likely to cause "voids" during extrusion. These "voids" will generate discontinuity within the fiber and limit the degree of post spinning extension (enhancing molecular alignment) and ultimately fiber strength.

Identification of a suitable buffer composition for maintaining protein solubility at high concentrations (300-500 mg/ml) was conducted through a series of dialysis and ultracentrifugation experiments. The most important factor to resolve is optimization of protein solubility within a broad concentration range to enhance protein recovery and minimize the introduction of defects in the fiber. In addition to aggregation, at very high protein concentrations gelation has been observed over time. It is therefore important to monitor this phase behavior as well.

Table 1. Summary of processing volumes and concentrations during the FLH dialysis study to evaluate the influence of glycine

Glycine (mM)[a]	Sample	Volume (µl)	Concentration (mg/ml)[b]
0	Supernatant	650	93.1
	CC10 retentate	100	512.9
10	Supernatant	500	75.1
	CC10 retentate	80	576.5
25	Supernatant	700	93.0
	CC10 retentate	150	508.5
50	Supernatant	500	119.7
	CC10 retentate	95	689.5
100	Supernatant	700	92.1
	CC10 retentate	100	508.6

[a]All samples were dialyzed into the spin buffer (160 mM urea, 10 mM $Na_2H_2PO_4$, 1 mM Tris, pH 5.0) supplemented with the indicated glycine concentration; [b]concentration was determined through the standard BCA protein assay with bovine serum albumin as the protein standard; CC10 retentate = soluble fraction resulting from concentrating with Centricon 10 (CC10) ultrafiltration systems

Homogenization and extraction of the lens proteins occurs in the following buffer: 50 mM Tris, 5 mM EDTA and 1 mM DTT, pH 7.5. We planned to follow methods utilized for spider silk fiber spinning. These involve protein solubilization followed by dialysis into the spin buffer (denaturing and non-denaturing conditions), ultrafiltration to concentrate the protein, and aging of sample to maximize intermolecular entanglements prior to spinning. Although this general process was successful for spinning crystallin proteins, significant modification of the buffer composition was necessary to maintain solubility and control gelation.

Direct dialysis into the silk spinning buffer (10 mM NaH_2PO_4, 1 mM Tris-HCl with and without supplementation of 160 mM urea) yielded a white, opaque solution indicative of significant amorphous aggregation. Several amino acids are known to disrupt aggregation including glycine, lysine and arginine. Below we describe a systematic study to investigate the role of each amino acid in protein solubility and gelation behavior.

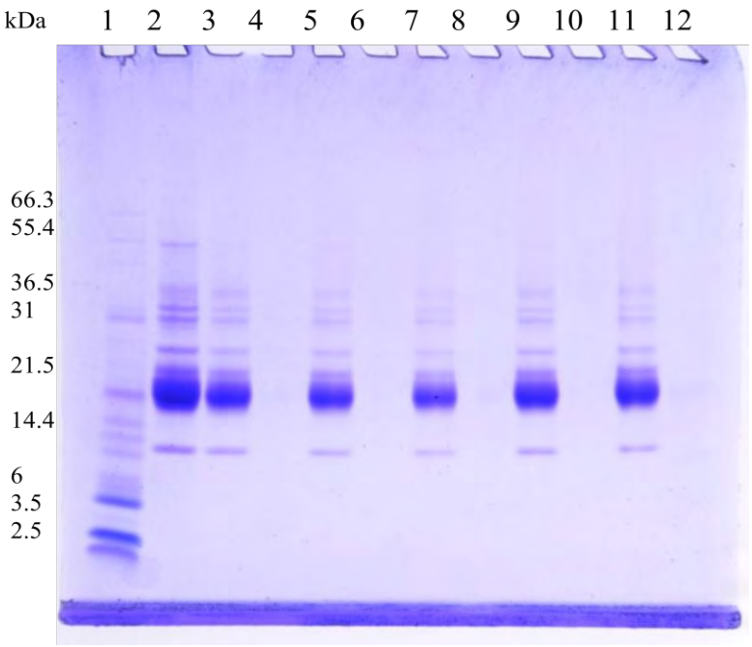

Figure 4. SDS-PAGE analysis of FLH dialysates concentrated with Centricon 10 (CC10) ultrafiltration systems. CC10 retentates were run on a 4-12% NuPAGE gel and visualized with Coomassie Blue stain. Lane 1: Mark 12 molecular weight standard (Invitrogen), in kDa; Lane 2: FLH (pre-dialysis); Lanes 3 & 4: FLH dialyzed into 0mM glycine retentate and filtrate; Lanes 5 & 6: FLH dialyzed into 10 mM glycine retentate and filtrate; Lanes 7 & 8: FLH dialyzed into 25 mM glycine retentate and filtrate; Lanes 9 & 10: FLH dialyzed into 50 mM glycine retentate and filtrate; Lanes 11 & 12: FLH dialyzed into 100 mM glycine retentate and filtrate. The glycine containing samples look similar to the 0 mM glycine control sample and the pre-dialysis sample.

Two approaches were taken to investigate glycine as a stabilizing buffer component: 1) dialysis into the spin buffer supplemented with a range of glycine concentrations (0-100 mM); and 2) FLH "spiked" with glycine (final concentration = 10 mM) directly prior to the concentration steps. In the first approach, FLH was dialyzed using 3500 molecular weight cutoff (MWCO) tubing into spin buffer supplemented with 160 mM urea and 0, 10, 25, 50 and 100 mM glycine. A dialysis procedure was designed to include several buffer exchanges and ensure equilibrium was reached and efficient buffer transfer was achieved. Because self-assembly and molecular aggregation are known to be kinetically driven, controlling the rate of dialysis is essential to this process. Post-dialysis samples (dialysates) clearly contained white, insoluble material. Insoluble material was removed by centrifugation and the supernatants were quantitated with a standard BCA protein assay and ranged from 75-120 mg/ml (Table 1). Clarified protein samples were then concentrated using ultrafiltration (CC10; 10,000 MWCO membrane-). The resulting retentates ranged between 80-150 µl, which corresponds to ~5-7 fold volume reduction. Protein concentrations of the CC10 rententates were determined to be ~510-690 mg/ml. Visual observations indicated that the samples appear more opaque as glycine concentration increases, similar to that seen with the dialysates. For all concentrated samples, precipitation was minimal during the CC10 processing, which was slightly unanticipated since protein self-association is more evident in concentrated solutions. As expected, solution viscosity also increased as the

samples became more concentrated and was accompanied by a biphasic solution. This biphasic solution consisted of a clear solution and slightly more viscous "slurry" that could be resuspended with gentle agitation. To understand the influence of glycine on the solubility of crystallin proteins, SDS-PAGE was performed. SDS-PAGE revealed that FLH consists of several proteins ranging from ~14-55 kDa (Figure 4). No observed differences between the FLH (pre-dialysis) sample and the retentates were evident. Although, distinct visual differences (i.e. opacity) were observed between the samples as glycine concentration increased. ***These results suggest that aggregation is present throughout all glycine concentrations in the silk spinning buffer including samples without glycine. The composition of the insoluble material is very similar or identical to that of the initial sample suggesting that aggregation is not driven by one specific protein in the sample. Furthermore, the presence of glycine in the buffer does not preferentially precipitate specific proteins.***

Subsequent characterization of the dialysates was not possible due to precipitation/gelation upon storage (~3 weeks at 4^{o}C). After ~2 weeks of storage, the retentates also gelled. Close visual observation of the dialysate samples indicated slight differences. The 0 mM glycine dialysate yielded a large white pellet. Glycine containing dialysates all presented a large white pellet similar to the control; however, a small soluble layer above the pellet was also observed. This may be indicative of some glycine influence; however, further investigation was necessary.

Table 2. Summary of FLH "spiked" glycine concentration study

Glycine (mM)	Sample	Volume (μl)	Concentration (mg/ml)[a]
0	FLH	900	157.1
	CC10 retentate	330	271.8
	MC10 retentate	40	n/a
10	FLH	930	175.5
	CC10 retentate	330	267.9
	MC10 retenate	60	n/a

[a]concentration was determined through the standard BCA protein assay with bovine serum albumin as the protein standard; CC10 retentate = final volume resulting from concentrating with Centricon 10 ultrafiltration systems; MC10 retenate = final volume resulting from concentrating with Microcon 10 ultrafiltration systems

In the 2nd approach to investigate glycine as a stabilizing component of the buffer, FLH in homogenization buffer (50 mM Tris, 1 mM EDTA, 1 mM DTT, pH 7.2) was concentrated in parallel with an FLH sample that was "spiked" with 1 M glycine to yield a final concentration of 10 mM. This approach introduced glycine without dialysis. The two samples were processed in parallel to determine the influence of glycine on protein stability during the concentration process. Sample volumes and resulting concentrations are listed in Table 2. Both samples underwent a ~2.5 fold volume reduction by ultrafiltration. Insoluble material was not evident in either sample; however, there was a "soft" viscous layer in both samples, as was previously seen. This soft layer was agitated to create a uniform solution. The sample volumes were further reduced 5-8 fold using MC10 ultrafiltration. The FLH took longer to concentrate than the FLH + 10 mM glycine. Once completed, the FLH was extremely viscous and gelled within minutes while the FLH + 10 mM glycine sample did not gel and was collected. Protein concentration of this sample could not be determined due to the high viscosity. Both

samples were analyzed by SDS-PAGE (data not presented herein as all samples appeared similar to those in Figure 4). Even the highly concentrated samples of FLH and FLH + glycine retained the same profile of proteins. A comparison of the FLH and FLH + glycine samples revealed minimal differences; however, observations during ultrafiltration clearly indicated differences in viscosity and phase behavior as the process evolved. ***These results suggest that glycine may enhance the solubility of proteins particularly for highly concentrated samples. However, the rate of gelation is faster than desired for processing of a spin dope and fiber spinning. Furthermore, the present solubility study suggests that solubility may be enhanced in the absence of the denaturant, urea, and/or the higher pH of the homogenization buffer.***

To further investigate the role of glycine, pH and denaturant on protein solubility the spider silk spinning buffer (10 mM $Na_2H_2PO_4$, 1 mM Tris, pH 5.0; abbreviated phosphate-tris (PT)) composition was modified by removing the denaturant urea and supplemented with a range of glycine concentrations between 0-100 mM. FLH was dialyzed into each of these buffers and centrifuged to remove any insoluble materials. All samples contained a white insoluble, gel-like pellet. Glycine containing samples were visually clear while the no glycine control still remained slightly opaque. SDS-PAGE analysis indicated minimal differences between the PT-0 mM glycine sample and those sample containing 10, 25, 50 and 100 mM glycine respectively (data not shown). This was expected based on previous gels.

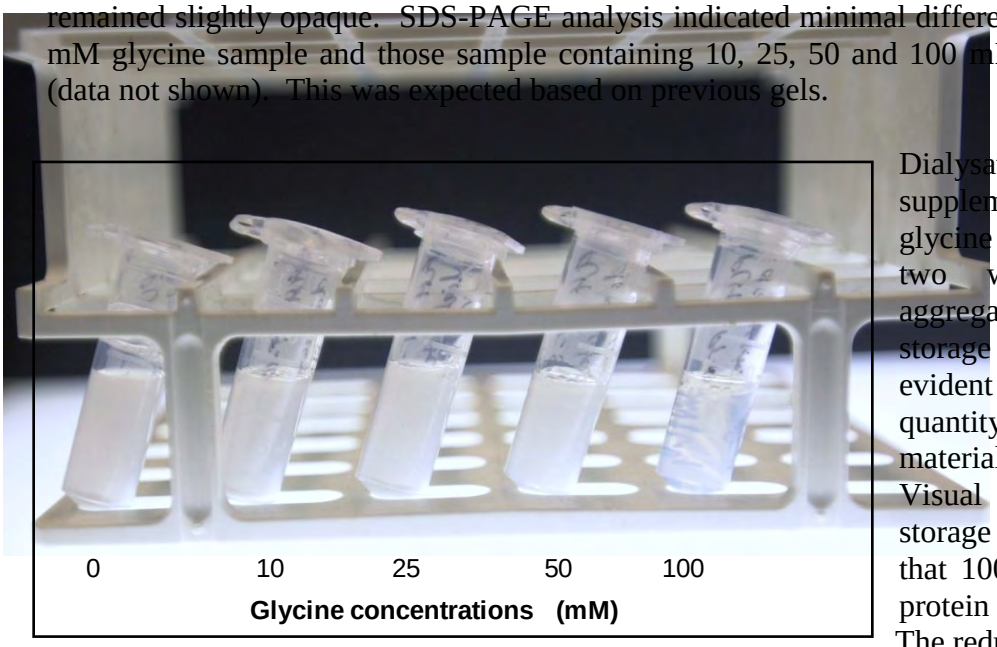

Figure 5. Visual observations of the influence of glycine on FLH aggregation. FLH dialysates in PT supplemented with 0-100mM glycine. After two weeks of storage at 4°C, white insolubles (i.e. aggregation) is visually evident in the 0 mM glycine control sample. Similar to the 0 mM glycine sample, 10 mM and 25 mM glycine had a large amount of aggregation. At 50 mM glycine, the amount of insolubles appeared less while the 100mM glycine had a significant reduction.

Dialysates prepared in PT supplemented with 0-100 mM glycine were stored at 4°C for two weeks. Significant aggregation occurs during storage at 4°C, which is evident by the increasing quantity of white insoluble material produced over time. Visual observations after storage clearly demonstrated that 100 mM glycine reduces protein aggregation (Figure 5). The reduction in aggregation is presumably due to glycine stabilizing the structure of the protein. A protein assay confirmed all samples were of similar concentration thereby indicating that glycine was indeed responsible for the reduced aggregation. These samples were further processed via ultrafiltration to final protein concentrations of estimated 500 mg/ml. The samples were spun with our aqueous processing procedures discussed below.

These studies confirm that the denaturant, urea induces aggregation. In all cases, dialysis into glycine containing buffers (particularly 100 mM) appeared to assist in controlling self-association, but the most dramatic effects were observed over extended periods of time (~2 weeks). In follow on studies discussed below, the direct addition of glycine appeared to perform better in coagulation while the enhancement of fiber coagulation was minimal relative to the no glycine control.

Due to inefficiencies of glycine for immediate influence on controlling protein self-association and self-assembly, arginine and lysine were investigated. These amino acids have the potential to address most observed requirements for enhancing protein solubility and fiber spinning. Arginine and lysine are basic, positively charged amino acids that have been shown in literature to stabilize protein self-association and increase non-covalent cross linking at high concentrations [35, 36]. The PT buffer was used as a control while modified buffers included PT supplemented with 0.2 M arginine (pH = 10.45) and PT supplemented with 0.2 M lysine-HCl (pH = 5.20). PT and PT-lysine dialysates were both very similar in appearance with a substantial amount of white insoluble material after centrifugation and cloudy supernatants. More specifically, the PT-lysine dialysate had three phases: (1) soluble protein, (2) cloudy suspension that would not pellet after extensive centrifugation and (3) white, insoluble material. This unique triphasic behavior is directly associated with the addition of lysine. Although this presents a fundamental intriguing result, it will not be investigated herein. In the dialysate containing arginine, the white insoluble material was no longer present and following centrifugation only a trace amount of insoluble material was present.

Table 3. Summary of processing volumes and concentrations during the processing of FLH in arginine containing aqueous spin buffer

FLH (batch)[a]	Arginine (mM)[b]	Sample	Volume (ml)	Concentration (mg/ml)[c]
FLH02	0.2	Pre-dialysis	1.5	273.9
		Post-dialysis	1.8	210.7
		CC10 retentate	0.8	291.0
FLH03	0.2	Pre-dialysis	1.5	201.1
		Post-dialysis	1.8	200.6
		CC10 retentate	0.8	275.5

[a]Processing batches are from the same homogenate (Lot 10-28-09) and represent a different processing date with identical processing conditions. [b]All samples were dialyzed into the spin buffer 10mM $Na_2H_2PO_4$, 1mM Tris supplemented with 0.2M arginine (final pH = 10.5); [c]concentration was determined through the standard BCA protein assay with bovine serum albumin as the protein standard; CC10 retentate = soluble fraction resulting from concentrating with Centricon 10 ultrafiltration systems

Additional studies were performed to investigate the effects of arginine concentration on solubility. Dialysis into PT buffer supplemented with 0, 0.2, 0.4 and 0.6 M arginine with a pH range from pH 10.4-10.6 was conducted. After dialysis, insoluble material was not present in the samples containing 0.2 and 0.4 M arginine while the sample with 0.6 M arginine produced a clear gel. ***This gelation event was a turning point in our research. An optically clear gel***

suggests that arginine is stabilizing the protein structure and participating in cross links which are necessary for successful fiber spinning. Further concentration of the soluble samples by ultrafiltration to an approximate concentration of 400-500 mg/ml produced a clear gel for the 0.4 M arginine containing sample and a highly viscous solution in the 0.2 M arginine buffer. However, coagulation testing (see details below) could not be conducted with the gelled samples. Therefore, subsequent processing of FLH in PT buffer supplemented with 0.2M arginine was performed and a reduced volume reduction during ultrafiltration was implemented. Spin dopes were reproducibly prepared at final concentrations of ~ 300 mg/ml (Table 3) and suitable (i.e. viscous but soluble) for coagulation studies. At this concentration, FLH was stable for approximately 2 days. Additional experiments were performed to scale up the solution processing allowing for a more systematic study of solution, spinning and post-spinning variables. The sample is typically stored for ~48 hrs prior to spin trials allowing sufficient self-assembly of the protein, which facilitates fiber formation. ***These results suggest that arginine is best suited for enhancing protein solubility, maximizing protein yield and fiber spinning. The pH of this preparation was much higher than previously investigated, which may have contributed to the improved solubility. Future work should evaluate the role of arginine in protein:protein interactions and non-covalent cross linking.***

Evaluation of coagulation and cross-linking agents for fiber spinning

Coagulation tests were performed in a range of buffer conditions and at varying points of the sample concentration and/or storage process to evaluate the role of these variables on fiber coagulation (i.e. formation). Briefly, a Hamilton syringe with 5-10 µl of sample is dispensed into a coagulation bath at a constant rate. A successful trial will yield a continuous fiber-like structure about ½ the distance to the bottom of the vial, which after 1-2 minutes of coagulation withstands mild agitation. Coagulation tests were typically performed in 40-60 % MeOH and 40-60% IPA; however, 70% IPA was occasionally evaluated as well.

FLH dialyzed into the PT-100 mM glycine buffer were initially evaluated prior to concentration (~130 mg/ml). The sample did not coagulate in 40% IPA. In 60% IPA, coagulation occurred immediately although the product was globular and lacking fibrous structure. In 50% IPA, fibers were formed near the bottom of the vial. The fibers easily broke up with gentle agitation. In MeOH, fibers were formed in all percentages tested; but all broke apart with gentle agitation suggesting the protein concentration may be too low.

To evaluate the impact of glycine concentration on coagulation, all samples were concentrated to approximately 500 mg/ml. Coagulation into a 50% MeOH bath was conducted with samples containing 0, 10, 25 50 and 100 mM glycine. Formation of a globular, non-fibrous structure was observed with samples containing 50 mM glycine or lower. The 100 mM glycine sample yielded fibers that were more defined and remained intact with agitation better than the 130 mg/ml coagulation tests. In 40% MeOH, both 50 and 100 mM glycine formed fibers; however, the 100 mM glycine sample had more intact fibers after gentle agitation. In 40% IPA, 50 mM and 100 mM glycine formed intact fibers after a brief delay (~15 s). At >40% IPA, coagulation was immediate; any fibers formed broke up easily. ***In summary, the coagulation results indicate that increasing glycine concentration facilitated coagulation. Also, the higher protein concentration produced better fibers in coagulation baths with a lower percentage of alcohol.***

As a result of the coagulation test, spin trials were conducted with PT-100 mM glycine samples in 50% MeOH and PT-50 mM glycine sample in both 40% and 50% MeOH (details presented below).

Coagulation tests were predominantly performed on samples dialyzed into PT- 0.2M arginine based on successful solubility studies presented in the previous section. Initial coagulation test were conducted with protein concentrations ranging from 400-500 mg/ml in a 50% or 60% MeOH coagulation bath. In both cases, coagulated fibers are initially clear but turn white after several minutes in the bath. Fibers were not as brittle as those seen with PT, PT-glycine or PT-lysine containing buffers since gentle agitation did disrupt the fiber-like structures. Furthermore several small pieces of fibers were strong enough to withstand removal from the 50% and 60% MeOH coagulation bath. Coagulation in 60% MeOH was quicker than 50% MeOH and resulted in shorter fibers with larger diameters and whiter in appearance. Coagulation in 50% and 60% IPA revealed similar fiber formation as that seen with MeOH except the fibers formed were typically longer. **In summary, the coagulation test results revealed that arginine containing buffers facilitate coagulation of fibers with more integrity than previously observed with PT or PT-glycine buffers. Interestingly, optimal coagulation occurs in a 60% IPA bath and coagulation time is influenced by protein concentration (e.g. higher protein concentrations result in a faster coagulation rate). As a result of the coagulation test, spin trials were conducted with ~400 mg/ml FLH in PT-0.2M arginine in both 50% MeOH and 60% IPA as well as a 300 mg/ml FLH in PT-0.2M arginine in 60% and 70% IPA.**

<u>Spinning of protein based fibers through aqueous spinning techniques</u>

Numerous spin trials have been conducted using our patented aqueous spinning techniques. Small scale aqueous-based protein spinning is typically performed by loading ~50 μl of sample into a spinneret that is designed to generate shear forces, which orient the protein molecules as they move through the elongated spinneret and induce fibril formation in a coagulation bath. The viscous spin dope (i.e. protein solution) is forced through PEEK tubing (minimum diameter = 0.006") at a constant rate to achieve this alignment and molecular orientation. At this scale, fibers are often manipulated by hand to investigate draw ratios, for collection and for post-spinning characterization. Figure 6 presents a photograph of our small scale spinning apparatus.

Figure 6. Aqueous spinning system is displayed with a coagulation bath and Harvard pump. Typically, a spin trial uses 50 ul of sample. After fiber formation, fibers are removed by hand with tweezers, if possible.

Fiber spinning trials were conducted with the conditions established through coagulation tests. For the PT-100 mM glycine samples, 50% MeOH was selected as the coagulation bath. As depicted in Figure 7, long, continuous fibers were formed, the fiber did not fold and adhere to itself (which is a problem if coagulation conditions were not optimal). Furthermore, the fibers were able to be extended or drawn within the bath using tweezers. However, if fibers remained in the bath for 10 minutes, they were too brittle to be removed for additional characterization. The PT-100 mM glycine sample was also spun after aging (presumably enhancing intermolecular association) for 4 days at 4^{o}C. The fibers turned white immediately in the 50% MeOH coagulation bath which is indicative of rapid coagulation. If coagulation occurs too quickly, fibers are often very brittle and cannot be removed from the bath.

Figure 7. Aqueous spinning of FLH PT-100 mM glycine sample (500 mg/ml) in 50% methanol. Long, continuous fibers were formed and the fibers could be pulled within the bath.

The majority of our spinning trials were conducted with PT-0.2 M arginine samples due to the superior solubility, clarity and self-assembly properties observed in this buffer. Numerous spin trails were conducted to investigate the following variables: coagulation bath composition (50% MeOH, 60% and 70% IPA), spinneret diameter (0.006" vs. 0.010"), coagulation time, draw, drying parameters and protein concentration (~300-500 mg/ml). A description of the most promising results is presented herein.

FLH in PT-0.2 M arginine at a final concentration of ~400 mg/ml (termed FLH01) was spun immediately after ultrafiltration (i.e. without aging via storage) into coagulation baths of 50% MeOH and 60% IPA. Fibers formed in the 50% MeOH coagulation bath remained tacky after extensive coagulation time, which is indicative of incomplete coagulation. In 60% IPA, thin, clear fibers up 4" in length were formed after 1-2 minutes in the bath (see Appendix III for summary). The fibers were amenable to manipulation for collection and were not tacky. In total, four fibers were collected by tweezers. Three of the fibers were removed from the coagulation bath and kept constrained and rinsed in a water bath before storage in air. The fourth fiber was placed directly from IPA into the storage container. As anticipated, the fiber, which was not washed with water adhered to the polystyrene surface and could not be retrieved for additional testing. ***These results demonstrate that washing in water is required to prevent adherence to surfaces and allow further manipulation of the fiber after collection.***

A slightly lower concentration of FLH in PT-0.2 M arginine, ~ 300 mg/ml (termed FLH02), was spun into a 60% and 70% IPA bath immediately after concentration as well as after aging for two days at 4^{o}C (for a complete summary, see Appendix III). The purpose of this study was to investigate the influence of protein concentration and aging on fiber properties. The freshly concentrated sample formed thin fibers up to several inches in length (60% IPA coagulation bath). After 5 minutes in the coagulation bath, fibers were collected. Although these fibers could be manipulated, they were not as durable as the fibers formed from the higher protein concentrations. Additional spin trials with longer coagulation times (up to 10 minutes) did not

enhance fiber durability. Transitioning to 70% IPA facilitated faster coagulation resulting in fibers with visible defects and more brittleness than those previously collected. In total, six short fibers were collected from low concentration spin trials of the non-aged sample.

The same sample was aged for two days at 4°C. Spin trials of the aged sample were conducted in 60% IPA using both 0.006" and 0.010" PEEK tubing. Fibers were allowed to coagulate between 5-10 minutes and compared to the freshly spun sample. Overall, fiber characteristics were significantly different than the freshly spun sample and more closely resembled those spun from higher protein concentrations. ***These results suggest that aging enhances the arginine induced non-covalent cross linking and that the process is kinetically driven. The optimal amount of crosslinking must be determined and will depend on the interaction of arginine concentration and length of storage.*** Numerous fibers were easily manipulated in the coagulation bath and readily collected and washed in a water bath prior to storage. More than half of the fibers were greater than 2" in length (Figure 8). In addition to the natural draw on the fibers due to overcoming the surface tension upon removal from the coagulation and water baths, several fibers were manually extended in IPA up to 1.5x their original length. Fibers spun with the larger diameter spinneret (0.010 inch) were slightly larger in diameter but otherwise behaved similarly to those spun from the narrower spinneret.

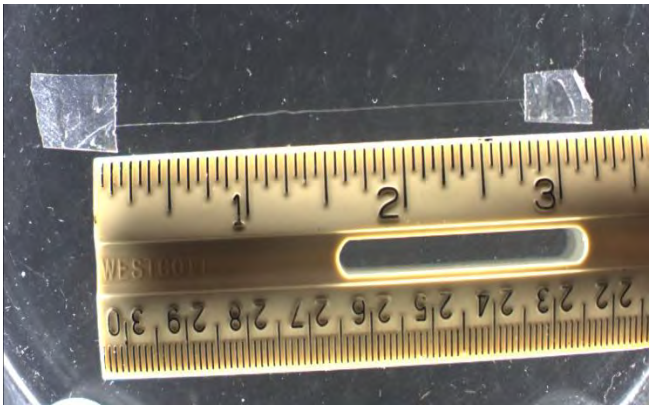

Figure 8. FLH fiber spun from a ~300 mg/ml solution in PT-0.2M arginine aged 2 days at 4°C. Fibers were sufficiently durable to handle after collection and prepared for optical and scanning electron microscopy.

Sample processing and spinning has been demonstrated to be reproducible. As a result, several spin trials were conducted using the concentrated scale-up procedures discussed previously. Based on experiences with previous spin trials and coagulation tests, the fibers were spun in 60% IPA from PT-0.2 M arginine (~275 mg/ml) using both 0.006" and 0.010" spinnerets (termed FLH03; for a complete summary, see Appendix III). As the fibers were extruded, the formed filament (clear fiber) was pulled the entire length of the bath to prevent agglomeration of the fibers at the bottom of the bath. This process resulted in formation of fibers of significant length (6-12"). Several fibers were collected undrawn for comparison to the FLH01 & FLH02 spin trials. Select fibers were drawn within the coagulation bath. The fibers exhibited elastic behavior and a small degree of extension (draw). Maximum draw was ~2-fold but typical draw was 1.5-fold. Beyond 2-fold, the fibers broke at defects introduced by the tweezers (i.e. edges of the fibers at which they are held for hand-drawing).

In combination, the three most recent spin trials (FLH01, FLH02 and FLH03) enabled a systematic analysis of solution (protein concentration and storage), spinning (spinneret diameter) and post-spinning (draw and coagulation time) variables. The variable analysis is summarized in Table 4. The variables were correlated to understand their role in fiber spinnability, diameter,

appearance, and molecular alignment. ***As a result of this analysis, it was determined that protein concentration and spin dope aging are dependent variables; increasing draw decreases fiber diameter but birefringence is unaffected and the optimal coagulation time is 15-20 min.*** Additional variable analyses are necessary.

Fiber Characterization and Variable Analysis									
Fiber	**Protein concentration (mg/ml)**	**Spin dope aging (hrs)**	**PEEK I.D. (in)**	**Draw (fold)**	**Draw solvent**	**Coagulation time (min)**	**Spun fiber length (in)**	**Avg. diameter (μm)**	**Birefringence**
FLH01-3	**388.5**	**2**	**.006**	**-----**	**-----**	**5**	**2**	**33.5**	**partial**
FLH02-5	**290**	**2**	**.006**	**-----**	**-----**	**7**	**0.5**	**28.5**	**partial**
FLH02-7	**290**	**47**	**.006**	**-----**	**-----**	**5**	**2**	**35.0**	**partial**
FLH02-9	**290**	**47**	**.006**	**-----**	**-----**	**15**	**2**	**38.5**	**Yes**
FLH02-17	**290**	**49**	**.010**	**-----**	**-----**	**15**	**1.5**	**33.5**	**Yes**
FLH03-4	**275**	**47**	**.006**	**2**	**IPA**	**15**	**2.5**	**23.5**	**No**
FLH03-7	**275**	**47**	**.006**	**1.5**	**IPA**	**25**	**1.5**	**28.0**	**Yes**
FLH03-9	**275**	**48**	**.010**	**2**	**IPA**	**5**	**1.5**	**20**	**partial**
FLH02-20	**290**	**49**	**.010**	**2**	**IPA**	**25**	**2**	**18.5**	**partial**

Table 4. Summary of FLH01, FLH02 and FLH03 spin trials. The columns in blue represent the systematic investigation of several important variables – protein concentration, storage, spinneret diameter, draw and coagulation time. While all other variables were held constant, one variable was changed to elucidate the role of the variable on fiber spinning, diameter, appearance, molecular alignment and mechanical integrity.

Characterization of FLH Fibers

The collected fibers have been characterized by polarizing light microscopy, SEM analysis and preliminary mechanical testing. Fiber diameter and birefringence of many samples have been measured by polarizing light microscopy under both common white light and polarizing light. Typically, in preparation for microscopy, the fibers must be removed from the sample container and taped to glass slides. Collected fibers exhibited sufficient durability for manipulation and flexibility when attempting to secure the fiber to glass slides. Figure 9 depicts optical microscope results of fiber FLH01-3. The image on the left (A) shows a common white light microscopy image of the fiber and the right (B) reveals the same fiber imaged with polarized light and a 530 nm tint plate. The blue color illustrates the birefrigent nature of the fiber and is indicative of molecular orientation along the fiber axis. The degree of birefringence is potentially an indicator of mechanical properties, based on previous experience with spider silk spinning. This fiber was analyzed prior to extension; therefore, it is anticipated that further alignment (birefringence) can be achieved upon single or double draw of fibers in the coagulation and water baths. For the first generation of scaled up processing and fiber spinning, these initial birefringent properties are promising. ***Although fibers exhibit molecular orientation as exhibited by birefringence, increasing draw (which decreases fiber diameter) did not affect birefringence. This suggests that the level of draw currently attained is not***

sufficient to result in increased orientation, and that further draw may improve orientation and fiber properties.

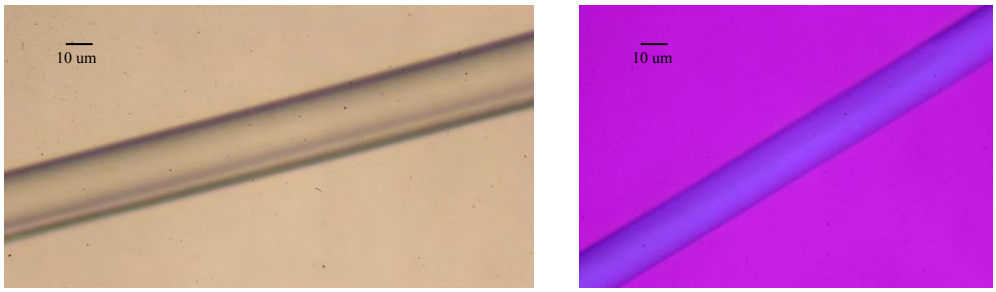

Figure 9. FLH01-3 (see table 4) characterized by light microscopy. A.) standard light image, which illustrates the consistent diameter of the fiber and the smooth nature at the fiber surface. FLH01-3, spun using 0.006" PEEK tubing in 60% isopropanol, was on average 33.25 um in diameter and exhibited minimal visual defects (i.e. fiber thinning, pits or breaks). B.) polarizing light to investigate birefringence using a 530 nm tint plate. FLH01-3 exhibited birefringence as indicated by the blue color upon using a tint plate.

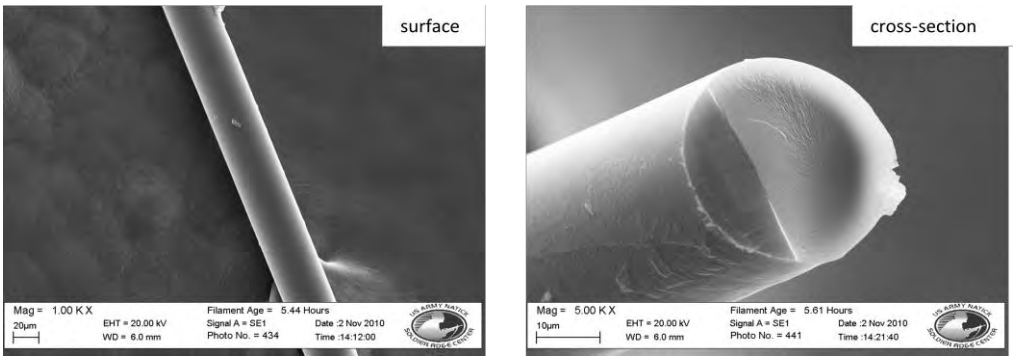

Figure 10. SEM of as-spun, undrawn fiber FLH02-14. The surface of the fiber is smooth and the inner core is solid. These images are representative of all the spun fibers.

Typical SEM images can be seen in Figure 10. The fibers, whether drawn or undrawn, exhibited a smooth surface and a solid interior core. SEM analysis revealed some common defects that were also prevalent in the light microscopy analysis. These include cracks along the length of some fibers, pits, thinning, bends and breakages. All of these defects influence the fiber's mechanical integrity and must be taken into consideration when transitioning to mechanical testing. Diameter thinning is particularly problematic since inclusion in the mechanical testing area would result in premature breakage at the thinned area, underestimating mechanical properties.

After microscopic analysis was completed and defects noted, select fibers were chosen for evaluation of mechanical properties. Criteria for selection were as follows: fibers > 1.5", defect-free region of the fiber for inclusion in testing area and ability to withstand pre-tension stress. Mechanical properties were determined on an Instron Model 55R4201 with a 2.5 N Load Cell

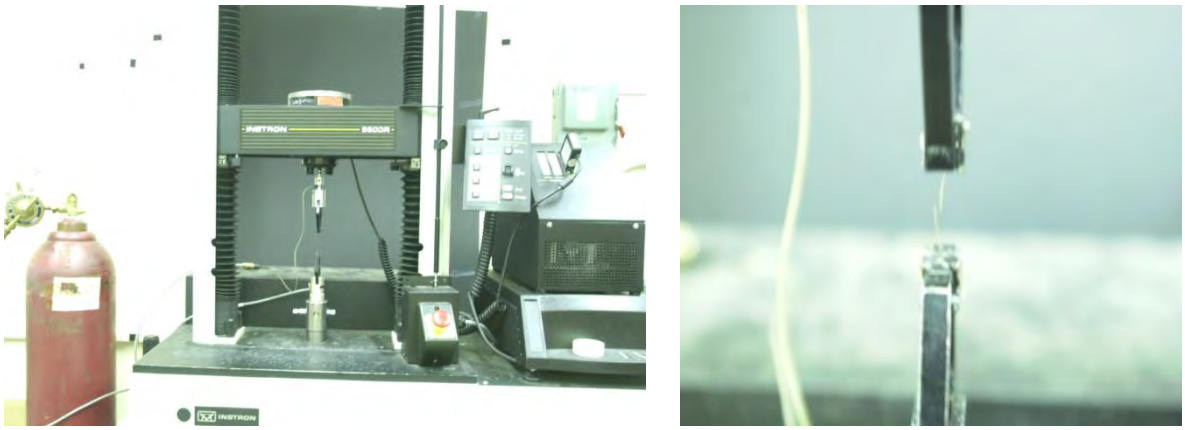

Figure 11. Instron mechanical testing system. Fibers are loaded into the pneumatic pinch grips. Using a 2.5 N Load Cell, the top grip is moved upward creating tension on the fiber. The fiber breaks under a certain load (an example can be seen in upper right image) and mechanical properties are recorded. Nine fibers were of the minimum required length (1.5 in) and sufficiently free of defects for testing; however, the fibers were too brittle to obtain measurable mechanical properties.

and pneumatic pinch grips that were closed with 50 psig nitrogen gas (Figure 11). Typical mechanical properties that were generated include: Maximum Load (g); Tenacity at Maximum Load (g/den); % Strain at Maximum Load (%); Displacement at break (mm); Tenacity at break (g/den); % Strain at break (%); Automatic Young's Modulus (g/den); Toughness (g/den). In total, 14 fibers were selected for mechanical testing from the three spin trials of FLH01, FLH02 and FLH03. However, due to fiber breakages during loading, only 9 fibers could be secured in the grips. Ideally, a load would be applied to the fibers with a crosshead speed (0.5 in/min or 12.7 mm/min) equivalent to the gauge length (0.5 in or 12.7 mm) and the fiber will break within the testing area (Figure 11, upper right). Unfortunately, in the case of all 9 fibers tested, the fibers broke at the pinch grips (termed jawbreak). This is due to the pneumatic closing of the grips and the pressure required for closure. The shock of the grips on the fiber broke the fiber in place. This is difficult to see until testing is concluded. The next generation of fibers may be evaluated with manual grips to avoid jawbreaks; although, a systematic analysis of solution and spinning variables that result in more durable fibers is necessary to achieve relevant mechanical properties.

Visual observations of the fibers suggest that the fibers became stiffer during storage. As-spun fibers, drawn or undrawn, displayed a degree of flexibility not unlike human hair. However, as the fibers were stored awaiting characterization and mechanical analysis, the flexibility was not as evident and the fibers became glossy in appearance. FLH01 was stored on the bench top while FLH02 and FLH03 fibers were stored in a humidity box at 55-60% relative humidity. In both cases, the stiffness of the fibers was evident. This phenomenon is most likely due to the arginine, which is essentially acting as a cross-linking agent to create fibers. A concentration study is necessary to optimize the arginine concentration that facilitates fiber formation but minimizes fiber stiffness during drying.

In summary, solid fibers exhibiting molecular orientation can be spun using this aqueous processing method. However, they are not of sufficient structure to allow the determination of

mechanical properties. These results suggest that the preparation of fiber spin solutions is not optimized to allow fibers to be sufficiently drawn to produce measureable mechanical properties. The optimal concentration of arginine must be determined to allow full protein solubilization as well as spin fibers that can undergo additional draw.

CONCLUSIONS & IMPLICATIONS FOR FUTURE RESEARCH

We have systematically evaluated the solubility characteristics and processing conditions necessary for the generation of protein based fibers from FLH waste materials. The eye lens crystallin proteins proved to be an excellent source of waste material yielding fibers of uniform molecular orientation and an average diameter of 35 μm. Furthermore, this aqueous based fiber spinning process is conducted at ambient temperatures with minimal energy demands thereby possessing the potential for a cradle to grave renewable, sustainable and environmentally friendly method.

Self-assembling systems, e.g. crystallin proteins, are driven by a delicate balance of thermodynamic and kinetic processes. When this balance is disrupted in a protein system, an unstructured and often recalcitrant molecular aggregate is generated. To capitalize on the benefits of self-assembling processes, minimize lose of material and inherent defects in the final product (fiber) it is important to understand the chemical environment capable of maintaining solubility at very high protein concentrations and encouraging formation of ordered molecular entanglements (gelation). As a result, significant effort was extended to identify the proper buffer composition and better control the assembly process prior to spinning. Buffer composition, pH, denaturant, and amino acid stabilizers were amongst the variables evaluated. Overall, our results suggest that the amino acid stabilizers influence phase behavior more the other variables investigated. Briefly, glycine enhances the solubility of crystallin proteins however; the rate of gelation is slower than that required for processing of spin dope and fiber spinning. Three distinct phases were produced in the presence of lysine; although this presents a fundamental intriguing result, it was not investigated further. Arginine produced the most dramatic effect with miniscule quantities of aggregation, the highest protein yield and production of an optically clear gel. The rate of gelation was dependent upon the concentration of arginine in the buffer. This gelation event was a turning point in our research. An optically clear gel suggests that arginine is stabilizing the protein structure and participating in cross links which are necessary for successful fiber spinning.

Numerous fibers were spun using this PT-arginine buffer to prepare a spin dope with enhanced stability and molecular order. The fibers were up to 12” in length and exhibited sufficient integrity for post-spinning manipulation and characterization. These fibers were reproducible in appearance and more robust than those produced in the absence of arginine. More importantly, the fibers possessed sufficient mechanical integrity to be manually drawn and removed from the coagulation bath. Solution, spinning and post-spinning variable analyses identified essential parameters that influence the formation of fibers with improved durability. It was determined that protein concentration and spin dope aging are dependent variables and the optimal coagulation time is 15-20 min. Fibers exhibited sufficient integrity for microscopic evaluation; however, mechanical properties were not obtained. Single fiber testing is an intricate and methodical process. Although the fibers were capable of manipulation, the current generation of fibers could not withstand the standard pneumatic grip closures at 50 psi during single fiber loading. Future mechanical testing will employ modified/manual grips and/or fiber stabilization approaches to conduct these measurements. Furthermore, additional characterization of the self-assembly process, spinning and post-spinning variables are anticipated to enhance fiber durability, which will also facilitate acquisition of mechanical properties.

Proof -of-principle has been confirmed for the spinning of eye lens crystallin proteins into fibers with mechanical integrity and reproducibility. Furthermore, environmental conditions which influence phase behavior are documented and will serve as a guide to direct more in depth investigations to correlate phase behavior at or before fiber spinning with mechanical and thermal properties of the produced fibers.

Previous spinning of silk and M13 bacteriophage has demonstrated the feasibility of achieving mechanical properties analogous to Nylon 6,6 (E= 1–3 GPa) and glassy homopolymers such as polystyrene (E= 2–4 GPa). We expect that fibers produced from waste protein sources are also capable of yielding similar mechanical properties. This is well aligned with the mission at NSRDEC as well as commodities within the commercial sector such as parachutes, fabrics, ropes and composite materials. Current manufacturing of nylon relies on the use of toxic diamines and diacids. In addition, approximately 95% of nylon production is conducted in China thereby creating a supply chain vulnerability for the U.S. military.

Continued research in this area has the potential to develop an environmentally safe manufacturing process with raw materials from waste products to replace Nylon 6,6. The work presented herein has confirmed that the diverse protein composition and distribution of proteins in the FLH does not change throughout the sample prep and spinning process. This demonstrates a remarkable tolerance and the feasibility of utilizing a homogenate thereby eliminating the need for costly, time consuming downstream protein purification.

Highly ordered molecular structures are required for fiber formation with mechanical integrity. Therefore it is important to better understand the assembly process which occurs while preparing the spin dope. Many ordered biological assemblies form liquid crystals at high concentrations (e.g. spider silk) or exhibit unique phase behavior. We have empirically observed these features in the PT-arginine samples and plan to utilize biophysical characterization methods such as static and dynamic light scattering, turbidity, differential scanning calorimetry, circular dichroism and infrared spectroscopy to obtain detailed information about aggregate size and shape, thermal stability and conformation. We will attempt to monitor these characteristics throughout the dialysis, concentration and storage to elucidate the role that buffer composition, protein concentration and time of storage have on aggregate size, thermal stability and conformation.

Understanding the role by which arginine contributes to these highly ordered structures will enable one to correlate supramolecular structure (in the spin dope) with the ultimate fiber properties. It was well established in the current studies that the concentration of arginine play an important role in phase behavior. We therefore plan to study are range of arginine concentrations to achieve an optimal concentration which will balance fiber formation and mechanical properties. Because this assembly process is kinetically driven, we also aim to investigate the temporal effects on aggregate size and shape, protein conformation and ultimately fiber characteristics. We will also utilize transmission electron microscopy to image the nanofibril morphology as a function of processing conditions.

A systematic analysis of processing and spinning variables that result in more durable fibers and correlation to protein self-assembly will be critical for producing stable spinning solutions capable of further draw. If draw can be increased sufficiently, fibers with improved mechanical

properties may be possible. We therefore recommend investigations which will introduce arginine into the coagulation bath and facilitate fiber coagulation (arginine may or may not be in spin dope). In addition, we will investigate the nano-reinforcement of fibers by introducing nanofibrils of known morphologies (analogous to those presented in Appendix II) into spin dopes prior to spinning. Spinning variables particularly draw (both single and double) will be correlated to mechanical properties. As previously mentioned, single fiber testing with modified grips and fiber stabilization techniques will be employed. Scale-up of spin dopes to facilitate automated fiber collection (take-up reel already designed and built) will be pursued. Finally, thermal properties, moisture uptake and the role of storage and post spinning treatments on mechanical and thermal properties will be explored.

PUBLICATIONS/PRESENTATIONS/OTHER PROFESSIONAL ACTIVITIES

1. Co-organization (Drs. Mello and Gerrard) of an international workshop entitled "Recent advances at the bio/abio interface" in Christchurch, New Zealand June 22nd-24th 2010.
2. "Identification of important process variables for fiber spinning of protein nanotubes generated from waste materials." C.M. Mello, J.W. Soares, and S.Arcidiacono SERDP Partnership Conference 2010.
3. "The higher ordered structures of protein nanofibres." M. Vasudevamurthy, J. Healy, K. Wong, and J. Gerrard. NanoIsrael 2010 conference in Tel Aviv

LITERATURE CITED

1. Mello, C.M. and Arcidiacono, S. (2003) Novel Purification & Fiber Spinning Techniques for Protein Fibers, *U.S. Patent 6,620,917*.
2. Lazaris, A., Arcidiacono, S., Huang, Y., Zhou , J.-F., Duguay, F., Chretien, N., Welsh, E.A., Soares, J.W. and Karatzas, C.N. (2002) Spider Silk Fibers Spun from Soluble Recombinant Silk Produced in Mammalian Cells, *Science* 295: 472-476.
3. Arcidiacono, S., Mello, C., Butler, M., Welsh, E., Soares, J. W., Ziegler, D., Allen, A., Laue, T., and Chase, S. (2002) Aqueous Processing and Fiber Spinning of Recombinant Spider Silks, *Macromolecules 35*, 1262-1266.
4. Oroudjev, E., Soares, J., Arcidiacono, A., Thompson, J.B., Fossey, S.A., and Hansma, H.G. (2002) Segmented nanofibers of spider dragline silk: Atomic force microscopy and single-molecule force spectroscopy, *Proceedings of the National Academy of Science* 99: 6460-6465.
5. Schreuder-Gibson, H.L., Mello, C.M., Albert, T., McManus, J.T., Dannemiller,D., Sennett, M.S. (2004) Electrospun Fibers and an Apparatus Therefor, *U.S. Patent 6,753,454.*
6. Chiang, C-Y, Mello, C. M., Gu, J., Van Vliet K., Belcher, A. M. (2007) Weaving Genetically Engineered Functionality into Mechanically Robust Virus Fibers, *Advanced Materials 19*, 826-832
7. Farsani, R. E., Shokuhfar A., Sedghi A. (2007) Conversion of modified commercial polyacrylonitrile fibers to carbon fibers, *International Journal of Mechanical Systems Science and Engineering 1,* 182-185.
8. Walsh P.J. (2001) *ASM Handbook- Composites,* ASM International, Ohio
9. Kostikov, V.I. (1995) *Fiber Science and Technology,* Chapman and Hall, London
10. Rajalingam, P. and Radhakrishnan, G. (1991) Polyacrylonitrile precursor for carbon fibers. *Polymer Reviews 31,* 301-310.
11. Chawla, K.K. (1998) *Fibrous Materials* Cambridge University Press Cambridge
12. Rowell, R.M., Sanadi, A.R., Caulfield, D.F., Jacobsen, R.E. (1997) Utilization of Natural Fibers in Plastic Composites: Problems and Opportunites, in *Lignocellulosic-Plastic Composites* (Leao, A.L., Carvalho, F.X., and Frollini, E., eds) pp. 23-51, USP, Brazil
13. Kandachur, P. and Brouwer, R. (2002) Applications of Bio-Composites in Industrial Products, *Materials Research Society Proceedings 702,* 1-12
14. Mohanty, A. K., Misra, M., Hinrichsen, G. Biofibres (2000) Biodegradable Polymers and Biocomposites: An overview. *Macromolecular Materials and Engineering,* 276-277(1):1-24
15. Mohanty, A. K., Misra, M., Drzal, L. T. (2002) Sustainable Bio-Composites from Renewable Resources: Opportunities and Challenges in the Green Materials World. *Journal of Polymers and Environment*, 10(1-2): 19-26
16. Mello, C. M., Soares, J. W., Arcidiacono, S., Butler, M. M. (2004) Acid Extraction and Purification of Recombinant Spider Silk Proteins, *Biomacromolecules* 5 (5): 1849-1852.
17. Arcidiacono, S., Mello, C. M., Kaplan, D., Cheley, S., Bayley, H. (1998). Purification and characterization of recombinant spider silk expressed in *Escherichia coli*. *Applied Microbiology and Biotechnology*, 49 (1), 31-38.
18. Fonoberov, V. A.; Balandin, A. A. (2004) Low-frequency vibrational modes of viruses used for nanoelectronic selfassemblies. *Phys. Status Solidi B 241*, R67 R69.

19. Nam, K. T.; Kim, D. W.; Yoo, P. J.; Chiang, C. Y.; Meethong, N.; Hammond, P. T.; Chiang, Y. M.; Belcher, A. M. (2006) Virus-enabled synthesis and assembly of nanowires for lithium ion battery electrodes. *Science 312*, 885 888.
20. Mao, C. B.; Solis, D. J.; Reiss, B. D.; Kottmann, S. T.; Sweeney, R. Y.; Hayhurs*t, A.; G***eorg**io*u,* G.; Iverson, B.; Belcher, A. M. (2004)Virus-based genetic toolkit for the directed synthesis of magnetic and semiconducting nanowires. *Science 303*, 213 217.
21. Lee, S. W.; Mao, C. B.; Flynn, C. E.; Belcher, A. M. (2002) Ordering of quantum dots using genetically engineered viruses. *Science 296*, 892 895.
22. Niu, Z. W.; Bruckman, M.; Kotakadi, V. S.; He, J.; Emrick, T.; Russell, T. P.; Yang, L.; Wang, Q. (2006) Study and characterization of tobacco mosaic virus head-to-tail assembly assisted by aniline polymerization. *Chem.Commun*. 3019 3021.
23. Niu, Z. W.; Bruckman, M. A.; Li, S. Q.; Lee, L. A.; Lee, B.; Pingali, S. V.; Thiyagarajan, P.; Wang, Q. (2007) Assembly of tobacco mosaic virus into fibrous and macroscopic bundled arrays mediated by surface aniline polymerization. *Langmuir 23*, 6719 6724.
24. Tseng, R. J.; Baker, C. O.; Shedd, B.; Huang, J. X.; Kaner, R. B.; Ouyang, J. Y.; Yang, Y. (2007) Charge transfer effect in the polyaniline-gold nanoparticle memory system. *Appl.Phys. Lett*. *90*, 053101.
25. Fonoberov, V. A.; Balandin, A. A. (2005) Phonon confinement effects in hybrid virus-inorganic nanotubes for nanoelectronic applications. *Nano Lett. 5*, 1920 1923.
26. Royston, E.; Lee, S. Y.; Culver, J. N.; Harris, M. T. (2006) Characte*rization of* **sil**ic*a*-coated tobacco mosaic virus. *J. Colloid Interface Sci. 298*, 706-712.
27. Bruckman, M. A.; Kaur, G.; Lee, L. A.; Xie, F.; Sepulveda,J.; Breitenkamp, R.; Zhang, X. F.; Joralemon, M.; Russell, T.P.; Emrick, T.; Wang, Q. (2008) Surface modification of tobacco mosaic virus with "click“ chemistry. *Chembiochem. 9*, 519-523.
28. Wang, Q., Lin, T. W., Tang, L., Johnson, J. E., and Finn, M. G. (2002) Icosahedral virus particles as addressable nanoscale building blocks. *Angew. Chem., Int. Ed.*, *41,* 459-462.
29. Wang, Q., Lin, T. W., Johnson, J. *E., and Fin*n, M. *G*. (2002) Natural supramolecular building blocks: Cysteine-added mutants of cowpea mosaic virus, *Chem. Biol*. *9*, 813-819.
30. Rong, J., Lee, A., Li, K., Harp, B., Mello, C.M., Niu, Z., and Wang, Q. (2008). Oriented cell growth on self-assembled bacteriophage M13 thin films. *Chemical Communications 41,* 5185-5187.
31. Garvey, M., Gras, S. L., Meehan, S., Meade, S. J., Carver, J. A., and Gerrard, J.A. (2009) Protein nanofibres of defined morphology prepared from mixtures of crude crystallins. *International Journal of Nanotechnology 6*, 258-73
32. Carver, J. A., Nicholls, K. A., Aquilina, J. A. and Truscott, R. J. (1996) Age-related changes in bovine alpha-crystallin and high-molecular-weight protein, *Experimental Eye Research 63*, 639-647.
33. Meehan, S., Berry, Y., Luisi, B., Dobson, C.M., Carver, J.A. and MacPhee, C.E. (2004) Amyloid fibril formation by lens crystallin proteins and its implications for cataract formation, *Journal of Biological Chemistry 279,* 3413-3419.
34. Zurdo, J., Guijarro, J. I. and Dobson, C. M. (2001) Preparation and characterization of purified amyloid fibrils, *Journal of the American Chemical Society 123* 8141-8142.
35. Das, U., Hariprasad, G., Ethayathulla, A.S., Manral, P., Das, T.K., Pasha, S., Mann, A., Ganguli, M., Verma, A.K., Bhat, R., Chandrayan, S.K., Ahemed, S., Sharma, S., Kaur, P., Singh, T.P., Srinivasan, A. (2007) Inhibition of protein aggregation: supramolecular assemblies of arginine hold the key. *PLos ONE* e1176.

36. Tsumoto, K., Umetsu, M., Kamagai, I., Ejima, D., Philo, J.S., Arakawa, T. (2004) Role of arginine in protein refolding, solubilization and purification. *Biotechnol Prog. 10*, 1301-1308.

APPENDICES

APPENDIX I
Survey of Important Variables for Coagulation and Fiber Spinning

A multivariate approach was utilized for the identification of important processing and spinning variables including soluble protein or nanofiber concentration, buffer compositions, coagulation or crosslinking bath composition, spinneret diameter, and temperature. Here we provide a synopsis of preliminary experiments to determine a suitable combination of protein/nanofiber concentration and coagulation/cross-linking bath composition required to produce fibers. Conditions which yielded fibers with sufficient mechanical integrity to withstand removal from a coagulation bath were selected and investigated systematically for the remainder of the program. Such conditions were defined as soluble fish lens homogenate spun into a coagulation bath in the absence of cross linker.

The table below reviews a range of sample preparation methods assessed for their ability to generate fibers. In addition, the effect of spinneret diameter was investigated with all producing similar effects. FLH at 67 mg/ml clogged the narrowest spinneret (10 µm) within a short period of time. Therefore all studies presented in the table were conducted with a spinneret diameter of 100 µm.

Sample preparation and coagulation assays

Sample prior to extrusion			**Coagulation results**	
Sample	Preparation	Visual characteristics	Extrusion solution	Visual characteristics
FLH 67 mg/ml[1]	None; stored at 4°C	Clear but visibly viscous solution[2]	45% MeOH	Precipitation into small, very brittle white fiber-like particles. Partly unformed.
FLH 67 mg/ml	None; stored at 4°C	Clear but visibly viscous solution	60% MeOH	Precipitation into small, very brittle white fiber-like particles
FLH 67 mg/ml	None; stored at 4°C	Clear but visibly viscous solution	70% MeOH	Precipitation into small, brittle fiber-like white particles
FLH 67 mg/ml	None; stored at 4°C	Clear but visibly viscous solution	80% MeOH	Precipitation into small, brittle fiber-like white particles
FLH 67 mg/ml	None; stored at 4°C	Clear but visibly viscous solution	90% MeOH	Precipitation into small, very brittle white fiber-like particles

FLH 67 mg/ml	None; stored at 4°C	Clear but visibly viscous solution	5% Glutaraldehyde	Precipitation into clear, fiber-like particles which slowly dissolved
FLH 67 mg/ml	None; stored at 4°C	Clear but visibly viscous solution	TFE 10%	Completely dissipated
FLH 67 mg/ml	None; stored at 4°C	Clear but visibly viscous solution	60% MeOH + 10% TFE	Precipitation into small, brittle fiber-like white particles
FLH 34 mg/ml; pH 7	Combined at room temperature	Clear solution	10% TFE	Completely dissipated
FLH 67 mg/ml; 10% TFE[3]; 0.66% HCl[4]	Combined at room temperature	Instant precipitation of white aggregates and viscous white semi-gel formation[5]	Methanol 90%	Some precipitation, no fiber-like particles observed
FLH 67 mg/ml; 10% TFE	Combined at room temperature, placed at 37°C for 12 hours	Formation of viscous white semi-gel after incubation	90% MeOH	Some precipitation, no fiber-like particles observed
FLH 67 mg/ml; 10% TFE	Combined at room temperature, placed at 60°C for 1 hour	Formation of viscous white semi-gel within 10 mins of start of incubation	90% MeOH	Some precipitation, no fiber-like particles observed
FLH 34 mg/ml; 10% TFE; pH 3.5	Combined at room temperature	Instant formation of clear gel, within 2sec for ½ solution, within 5 mins for remainder of solution[6]	90% MeOH	Precipitation into small, very brittle fiber-like particles
FLH 34 mg/ml; 10% TFE; pH 3.5	Combined at room temperature	Instant formation of clear gel, within 2sec for ½ solution, within 5 mins for remainder of solution	8% Glutaraldehyde	Completely dissipated
FLH 7 mg/ml; 5% TFE; pH 3	Combined at room temperature	Clear solution	60% MeOH	Completely dissipated
FLH 7 mg/ml; 5% TFE; pH 3	Combined at room temperature	Clear solution	90% MeOH	Completely dissipated

FLH 7 mg/ml; 5% TFE; pH 3	Combined at room temperature	Clear solution	8% Glutaraldehyde	Precipitated into white non-fiber-like fragments
FLH 7 mg/ml; 5% TFE; pH 3	Combined at room temperature	Clear solution	5% Glutaraldehyde	Precipitated into clear non-fiber-like fragments
FLH 34 mg/ml; 5% TFE; pH 3.5	Combined at room temperature	Within 10 minutes began to form into a clear gel	8% Glutaraldehyde	Precipitated into clear non-fiber-like fragments
FLH 67 mg/ml; spiked with fibril seeds[7]	Incubated at 60°C	Formed white semi-gel within 5 minutes. Not used for coagulation tests	-	-
FLH 67 mg/ml; spiked with fibril pseudo-seeds[5]	Incubated at 37°C for 10 mins	Clear solution	70% MeOH	Precipitation into small, very brittle fiber-like particles
FLH 67 mg/ml; spiked with low concentration fibrils[8]	Incubated at 37°C for 10 mins	Clear solution	70% MeOH	Precipitation into small, very brittle fiber-like particles
FLH 67 mg/ml; pH 2 (1% HCl)	Incubated at 37°C for 10 mins	pH 2 addition formed immediate white aggregates; incubation of remaining solution formed clear gel within 10 minutes	70% MeOH	Precipitated into clear non-fiber-like fragments
FLH 67 mg/l; pH 2 (1% conc. HCl)	Incubated at 37°C for 10 mins	Ph 2 addition formed immediate white aggregates; incubation of remaining solution formed clear gel within 10 minutes	5% Glutaraldehyde	Precipitated into clear non-fiber-like fragments

[1] FLH concentrations are final concentration used. Dilutions were achieved with water at either neutral pH or pH 2. As a consequence, Tris buffer concentrations in these solutions range from between 5 to 50 mM. Accurate buffer composition will be provided for all solutions which show promising results.
[2] Any particles not in solution were spun prior to assay. Higher concentrations lead to increased particulate matter in FLH solutions
[3] Trifluoroethanol (TFE)

[4]*Hydrochloric acid (HCl)*
[5]*Potentially an amorphously aggregated solution, based on previous X-ray Diffraction (XRD) results (not conducted on these samples) for clear vs white crystallin fibril stalks (clear stalks showing high β-sheet, white stalks causing random radiation patterns)*
[6]*Potentially a highly ordered β-sheet solution, based on XRD results for clear vs white crystallin fibril stalks (clear stalks showing high β-sheet, white stalks causing random radiation patterns)*
[7]*Clear gel solutions formed instantly on the addition of pH 2 water and TFE to FLH (34 mg/ml) were diluted 1:1 in water and sonicated for 50 min on high until gel was completely re-solubilised.*
[8]*Fibril solutions prepared from Baracuda FLH at ~6 mg/ml pH 3 incubated with 10% TFE for 24hrs then at room temperature for 1 week. Transmission electron microscopy (TEM) has shown fibrils and ribbon structures present in sample. Samples were spun at 14'500 rpm for 30 min to remove large aggregates. Supernatant was used as low-concentration fibril solution.*

Conclusions drawn from these studies assisted in focusing our experimental approach. These initial trials with FLH have produced viscous samples amenable to processing. The most successful coagulation trials with FLH were extruded into 70-80% MeOH. At higher protein concentrations it is also thought that some successful results with glutaraldehyde cross linking may also be observed (see Appendix III).

Increasing protein concentration appears to be important for both coagulation into an alcohol bath and crosslinking with glutaraldehyde. Experiments were conducted to compare the effectiveness of C-3 and C-10 amicon ultrafiltration devices for sample concentration. Both filters retained FLH in a similar manner while the C-10 devices resulted in a faster rate. All subsequent studies with FLH (or soluble protein) were conducted with the C-10. Alternatively, concentrating pre-formed fibrils, for extrusion and cross-linking experiments revealed that C-3 filters are significantly more effective at retaining fibrils than C-10. However, in both devices the formation of a fibril mat-like aggregate over the filter membrane creates a technical hurdle which must be addressed in future work.

APPENDIX II
Optimization of fibril synthesis

The original proposal presented two very different fiber spinning strategies of spinning from soluble protein homogenates (presented in the body of this report) and nanofiber preparations (summarized herein). Initially, protein nanofibers (10-15nm in length) were prepared from soluble crystallin proteins using published methods. Preliminary coagulation trials with this standard preparation of fibrils were not as successful as those with FLH (presented in Appendix I). As a result, variables were explored and subsequently identified to control nanofibril length, degree of branching and bundling; all of which are thought to improve molecular entanglements and macroscopic assembly features. These interactions are essential for the formation of fibers and associated mechanical properties.

Building on published methods from Garvey *et al.*, the effects of temperature, incubation time, filtering steps and pH on improving the length of the fibrils was explored. In all cases, the samples were prepared from FLH was diluted to a concentration of approximately 10 mg/ml and dialyzed into distilled deionized water. Upon completion of the dialysis, insoluble protein was removed by centrifugation and the remaining supernatant was adjusted to pH 2 with HCl. TFE was added to a final concentration of 10% (v/v) and the sample was incubated and heated for a defined period of time. Typical TEM images obtained from various iterations of the method are included below.

Method 1 - Fibrils were prepared at 60^{o}C for 24 hours followed by incubation at room temperature for one week. ***The final product still had some aggregates and might have crystallins in non-fibrillar form.***

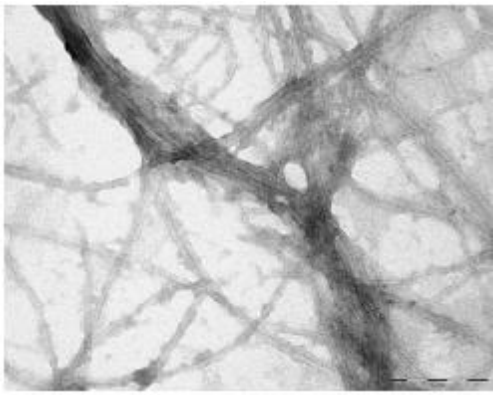

Method 2 - Fibrils were prepared at 60^{o}C for 1 hour while the centrifugation step to remove aggregates was conducted after 24 hour incubation at room temperature. Additional one week incubation at room temperature took place after centrifugation. ***Fibrils were approximately 1µm in length (orginal method – 15nm). This method also resulted in a clearer product without amorphous aggregates as is evident by the improved clarity of the samples. The delayed centrifugation step was therefore incorporated into all subsequent preparations.***

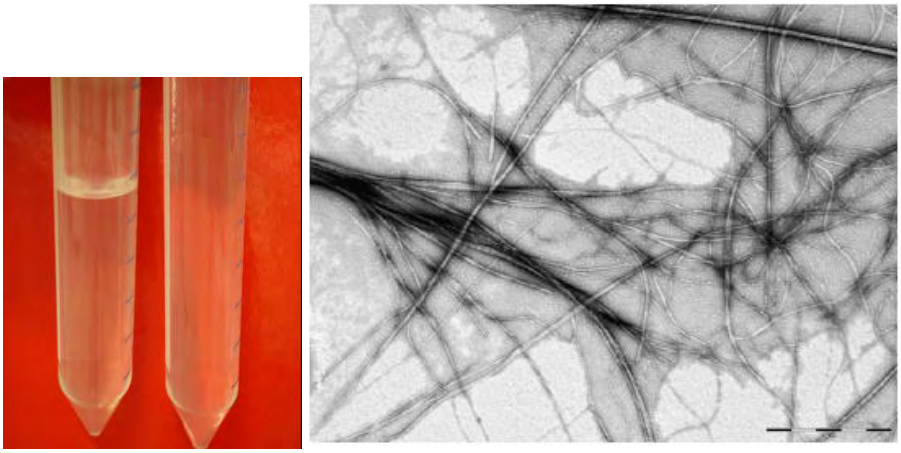

Method 3 - Similar to that of method 2, except the temperature of incubation was increased to 75^{o}C. Both images were taken from the same sample where left image (14K magnification) reveals the extended length and limited branching and the right image (89K magnification) clearly depicts the central bundling of the fibers. ***The fibrils are longer in length (up to 4µm) and seem to come together to form a core of bundles.***

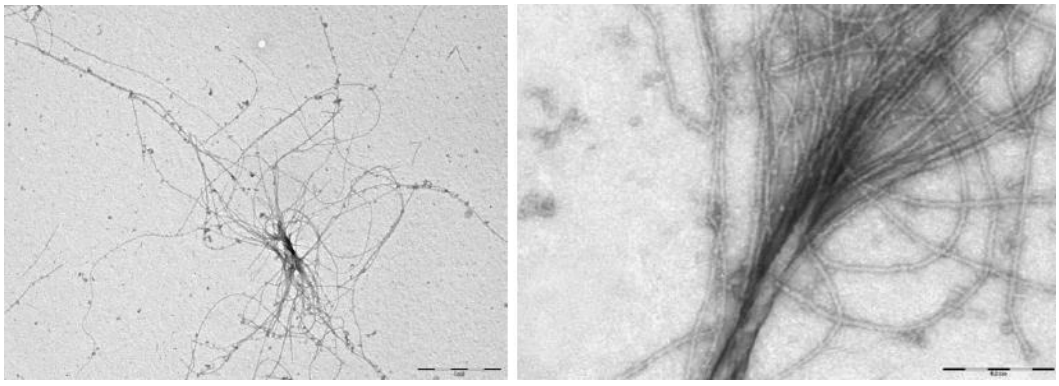

Method 4 - Similar to that of methods 2 & 3, except the temperature of incubation was increased to 85^{o}C. Both images were taken from the same sample where left image (14K magnification) reveals the extended length and increased branching and the right image (89K magnification) clearly depicts significant bundling of the fibers in the center of the supramolecular assembly. ***Increasing temperature resulted in higher yields and the individual fibril length was up to 5µm (see images below) and the fibrils are forming a larger core of bundles compared to method 3.***

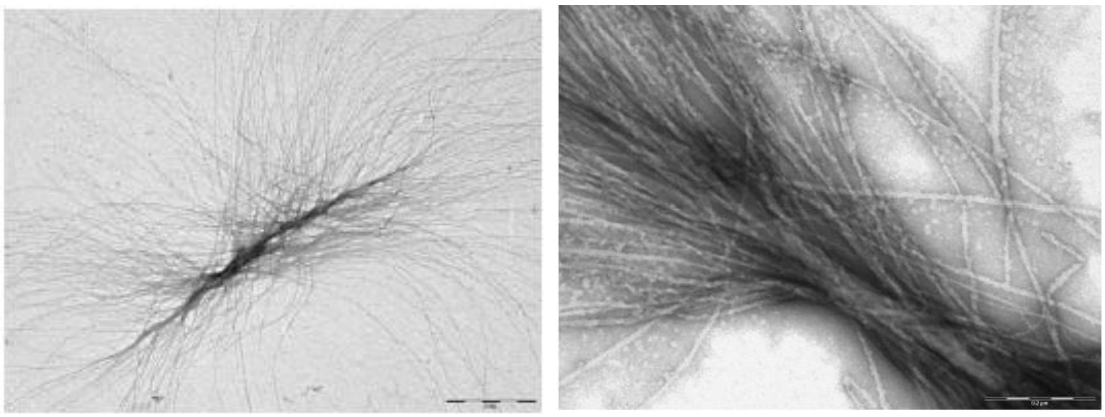

Method 5 - Similar to that of methods 2 & 3, except the temperature of incubation was increased to 90^{o}C. This method resulted in enhanced fibril branching with a number of intertwining bundles. Some of the largest branches are approximately 10 µm in length (see images below)

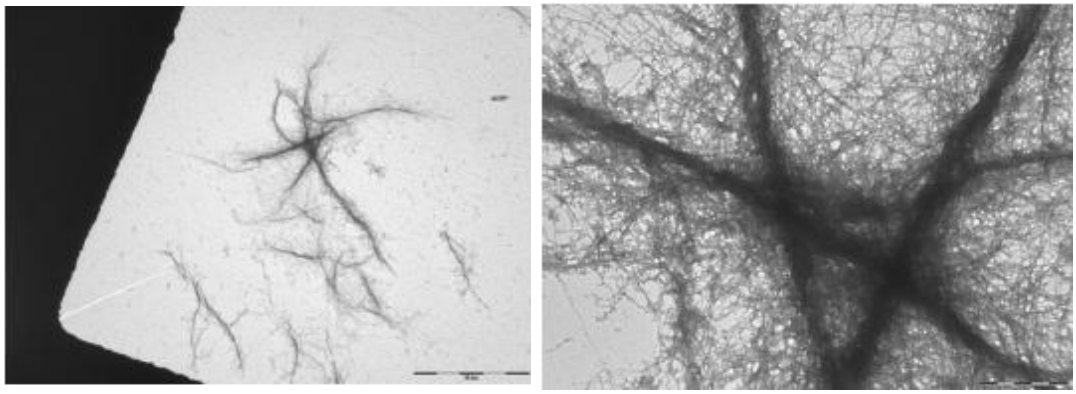

In summary, these data demonstrate that a significant enhancement in fibril length (15nm to 10µm) has been achieved compared to previously published data. Furthermore, the ability to control nanofibril length, morphology, degree of bundling and branching has been demonstrated. The determination of processing conditions to tailor and control these characteristics is a significant accomplishment which can lead to improved fiber properties. We aim to propose in a follow on effort experiments to investigate the concentration and spinning of these supramolecular assemblies. In addition, we plan to dope FLH with defined nanofibril morphologies from methods 4 and 5 to evaluate the impact of bundling and branching nanostructures on spinning of soluble proteins. Nano-reinforcement of materials has demonstrated a significant increase in strength with little added weight.

Appendix III

The Tables below describe in detail fibers created during spin trials FLH 01, FLH 02 and FLH 03. The tables consist of the solution, spinning and post-spinning conditions in which the fibers were formed and also the microscopic information acquired for each fiber. When summarized in total, ~40 fibers were spun with typical lengths of 1.5-2". Select fibers could be single drawn (i.e. drawn in coagulation bath) up to 2 fold draw but more typical was 1.5x the original length. All fibers were submersed in water prior to collection and dried as indicated. All fibers were analyzed microscopically under both common white light and polarizing conditions. Under common white light, fibers were investigated for defects such as breaks, pits, cracks, bend and diameter thinning. Under polarizing light, fibers molecular alignment was investigated by visually observing birefringence along the length of a fiber, typically using a 530 red tint plate. Average fiber diameter was also acquired during microscopic analysis with a minimum of five reading along the length of the fiber. Digital images of all fibers were obtained and recorded. The tables below summarize those observations for each fiber. Fibers were selected for mechanical testing if they were a minimum of 1.5 inches long and encompassed a ½ region that was defect free, preferably centrally located within the fiber. This area would become the gauge length or testing area during mechanical analysis.

Analysis of the combined spin trials enables a systematic evaluation of solution (protein concentration and storage), spinning (spinneret diameter) and post-spinning (draw and coagulation time) variables. Final variable analysis revealed protein concentration and spin dope aging were dependent variables; increasing draw decreases fiber diameter but birefringence is unaffected and the optimal coagulation time is 15-20 min. These conclusions will be the basis for the next generation spin trials.

Detailed summaries of each spin trial can be found below.

SUMMARY OF FLH01: Fibers were spun from a ~400 mg/ml PT/0.2M arginine solution immediately after concentrating. All fibers spun in a 60% IPA coagulation bath from a 0.006"spinerette at a constant spin rate, left in the bath a certain amount of time then collected after submersion in water. All fibers were collected undrawn after submersion in a water bath. Only FLH03-1 was analyzed microscopically; the other fibers broke during transfer to glass slides.

FLH01 summary of solution/spinning conditions						
Fiber	**spin (date-time)**	**FLH conc (mg/ml)**	**Volume (μl)**	**IPA (%)**	**PEEK ID (inches)**	**Spin rate (ml/min on pump)**
FLH01-1	10/1/10 - 1530	388.5	30	60%	0.006	0.007
FLH01-2	10/1/10 - 1550	388.5	35	60%	0.006	0.005
FLH01-3	10/1/10 - 1615	388.5	75	60%	0.006	0.005
FLH01-4	10/1/10 - 1615	388.5	75	60%	0.006	0.005

FLH01 summary of post-spinning manipulation and microscopic observations/evaluations

Fiber	removal	Draw (fold)	Draw solvent	Dried	Coag (min)	Observations (visual and microscopic)	Diameter range (μm)	Birefringence
FLH01-1	IPA to water	n/a	n/a	U	1-2	short, white	n/a	n/a
FLH01-2	IPA	n/a	n/a	U	1-2	1 tweezer removal; stuck to plate	n/a	n/a
FLH01-3	IPA to water	n/a	n/a	U	5-10	2"; durable, able to manipulate	29-38.8	partial (before bend)
FLH01-4	IPA to water	n/a	n/a	U	5-10	1.5"; durable, seam in fiber	n/a	Yes

Fibers analyzed on Nikon OptiPhoto 1 polarizing microscope, unless indicated as n/a under birefringence; U= unconstrained; C = constrained; coag = coagulation time

SUMMARY OF FLH 02: Fibers were spun from a 290 mg/ml PT/0.2M arginine solution immediately after concentrating and after ~48hrs of storage at 4°C. Two PEEK ID's were investigated with minimal change in spin rate. All fibers spun in a 60% IPA coagulation bath and collected after submersion in water. Coagulation time (time in IPA/water) varied as indicated. The majority of the fibers were collected undrawn although three were drawn up to 2-fold draw. All fibers analyzed microscopically and visual observations are summarized.

FLH02 summary of solution/spinning conditions						
Fiber	spin (date-time)	FLH conc (mg/ml)	Volume (μl)	IPA (%)	PEEK ID (inches)	Spin rate (ml/min on pump)
FLH02-1	10/5/10 - 1500	290	50	60%	0.006	0.007
FLH02-2	10/5/10 - 1500	290	50	60%	0.006	0.007
FLH02-3	10/5/10 - 1530	290	75	60%	0.006	0.007
FLH02-4	10/5/10 - 1550	290	75	70%	0.006	0.005
FLH02-5	10/5/10 - 1550	290	75	70%	0.006	0.005
FLH02-6	10/5/10 - 1610	290	75	60%	0.006	0.005
FLH02-7	10/7/10 - 1400	290	50	60%	0.006	0.005
FLH02-8	10/7/10 - 1400	290	50	60%	0.006	0.005
FLH02-9	10/7/10 - 1400	290	50	60%	0.006	0.005
FLH02-10	10/7/10 - 1400	290	50	60%	0.006	0.005
FLH02-11	10/7/10 - 1530	290	50	60%	0.006	0.005
FLH02-12	10/7/10 - 1530	290	50	60%	0.006	0.005
FLH02-13	10/7/10 - 1530	290	50	60%	0.006	0.005
FLH02-14	10/7/10 - 1530	290	50	60%	0.006	0.005
FLH02-15	10/7/10 - 1600	290	50	60%	0.010	0.005
FLH02-16	10/7/10 - 1600	290	50	60%	0.010	0.005
FLH02-17	10/7/10 - 1600	290	50	60%	0.010	0.005
FLH02-18	10/7/10 - 1600	290	50	60%	0.010	0.005
FLH02-19	10/7/10 - 1600	290	50	60%	0.010	0.005
FLH02-20	10/7/10 - 1600	290	50	60%	0.010	0.005

FLH 02 summary of post-spinning manipulation and microscopic observations/evaluations								
Fiber	removal	Draw	Draw	Dried	Coag	Observations (visual	Diameter	Birefringence

		(fold)	solvent		(min)	and microscopic)	range (μm)	
FLH02-1	IPA to water	n/a	n/a	U	5	slightly white; a bit tacky; no defects	~29	No
FLH02-2	IPA to water	n/a	n/a	U	5-10	single tweezer collect; slightly tacky, broke	n/a	n/a
FLH02-3	IPA to water	n/a	n/a	U	5	short fiber, tacky, not fully coag; defects	~24-29	No
FLH02-4	IPA to water	n/a	n/a	U	5	<0.25", twisting, necking; coag too quickly	~29-38	faint (no Δ at neck)
FLH02-5	IPA to water	n/a	n/a	U	7	0.5", visible defects, necking; coag too quickly	~19-38	partial (thin area)
FLH02-6	IPA to water	n/a	n/a	U	10	short fiber, bent back w/o break, loop	~29	No
FLH02-7	IPA to water	n/a	n/a	U	5	2", non-tacky, durable, slight defects	~21-58	partial
FLH02-8	IPA to water	n/a	n/a	U	5-10	2", non-tacky, durable	~19-53	partial
FLH02-9	IPA to water	n/a	n/a	U	10-15	2", non-tacky, durable, necking (49-29μm)	~29-58(A); 19-29(B)	9A-Yes; 9B-partial
FLH02-10	IPA to water	2	IPA	U	15-20	stretchy, uneven draw, break at 29μm	~14-44	partial
FLH02-11	IPA to water	n/a	n/a	U	10	1", durable, slight defects, necking, slit	~19-36	partial
FLH02-12	IPA to water	n/a	n/a	U	10-15	1", durable; B-bend; diam inc. after bend	~19(A); ~19-38(B)	12A-no; 12B-no
FLH02-13	IPA to water	1.5	IPA	C	10-15	0.75", draw on left side only (break side); "halo"	~19-38(A); 38-58(B)	13A-Yes; 13B-Yes
FLH02-14	IPA to water	n/a	n/a	U	15-20	1", durable; thin (< birefringence)	~34-80	Yes
FLH02-15	IPA to water	n/a	n/a	U	10	1.5", durable; necking	~15-40	partial
FLH02-16	IPA to water	n/a	n/a	U	10-15	1", durable; no defects	~19-26(A); 16-24(B)	16A-no; 16B-partial
FLH02-17	IPA to water	n/a	n/a	U	10-15	1", durable, slight (A) to no (B) defects	~19-48(A); ~46 (B)	17A-partial; 17B-Yes
FLH02-18	IPA to water	n/a	n/a	U	15-20	<1", broke; tweezer flattening	~39 (A&B)	18A-Yes; 18B-Yes
FLH02-19	IPA to water	n/a	n/a	U	15-20	1", durable; necking, defects	~19-38	partial
FLH02-20	IPA to water	2	IPA	C	20-25	broke at 2x, thinner at break, uneven draw	~14-27(A); 10-14(B)	20A-Yes; 20B-No

Fibers analyzed on Nikon OptiPhoto 1 polarizing microscope, unless indicated as n/a under birefringence;In cases where fiber broke during transfer to glass slides, indicated as A & B; U= unconstrained; C = constrained; coag = coagulation time

SUMMARYOF FLH03: Fibers were spun from a 275 mg/ml PT/0.2M arginine solution immediately after concentrating and after ~48hrs of storage at 4°C. Two PEEK ID were investigated at a constant spin rate. All fibers spun in a 60% IPA coagulation bath, left in the bath a certain amount of time then collected after submersion in water. The majority of the fibers were drawn up to 2-fold, although more typical was 1.5 fold draw. Some fibers were susceptible to additional draw but broke prior to collection and therefore are not part of this analysis. All fibers analyzed microscopically and visual observations are summarized.

FLH03 summary of solution/spinning conditions						
Fiber	**spin (date-time)**	**FLH conc (mg/ml)**	**Volume (μl)**	**IPA (%)**	**PEEK ID (inches)**	**Spin rate (ml/min on pump)**
FLH03-1	11/3/10 - 1500	275	50	60%	0.006	0.005
FLH03-2	11/3/10 - 1540	275	50	60%	0.006	0.005
FLH03-3	11/5/10 - 1410	275	50	60%	0.006	0.005
FLH03-4	11/5/10 - 1410	275	50	60%	0.006	0.005
FLH03-5	11/5/10 - 1410	275	50	60%	0.006	0.005
FLH03-6	11/5/10 - 1410	275	50	60%	0.006	0.005
FLH03-7	11/5/10 - 1410	275	50	60%	0.006	0.005
FLH03-8	11/5/10 - 1410	275	50	60%	0.006	0.005
FLH03-9	11/5/10 - 1510	275	50	60%	0.010	0.005
FLH03-10	11/5/10 - 1510	275	50	60%	0.010	0.005
FLH03-11	11/5/10 - 1510	275	50	60%	0.010	0.005
FLH03-12	11/5/10 - 1510	275	50	60%	0.010	0.005
FLH03-13	11/5/10 - 1600	275	50	60%	0.010	0.005

FLH03 summary of post-spinning manipulation and microscopic observations/evaluations								
Fiber	**removal**	**Draw (fold)**	**Draw solvent**	**Dried**	**Coag (min)**	**Observations (visual and microscopic)**	**Diameter range (μm)**	**Birefringence**
FLH03-1	IPA to water	n/a	n/a	U	25	short fiber, difficult to grip	n/a	n/a
FLH03-2	IPA to water	n/a	n/a	U	17	short fiber, not durable	n/a	n/a
FLH03-3	IPA to water	n/a	n/a	U	10	1.5"; brittle in sections, visible necking	27-34	partial
FLH03-4	IPA to water	2	IPA	U	15	2.5"; consistent D, no defects	20-27	no
FLH03-5	IPA to water	1.5	IPA	U	15	broke during transfer to glass	n/a	n/a
FLH03-6	IPA to water	n/a	n/a	C	20	brittle, broke into 3 pieces on transfer	27(A); 20(B)	no
FLH03-7	IPA to water	1.5	IPA	C	25	D decreases left to right	17-40	partial
FLH03-8	IPA to water	1.5	IPA	C	30	no major defects but large D increase left ot right	20-60	no

FLH03-9	IPA to water	2	IPA	C	5	1.5"; portion was stiff, inconsistent stretching	13-27	partial
FLH03-10	IPA to water	n/a	n/a	C	10	stuck to plate, could not be transferred	n/a	n/a
FLH03-11	IPA to water	1.5	IPA	C	25	fiber broke in middle during transfer	14-27(A); 20-34(B)	no
FLH03-12	IPA to water	1.5	IPA	C	30	no visible defects, consistent D	8-14	no
FLH03-13	IPA to water	1.5	IPA	U	15	broke, pts annotated, stuck to plate	n/a	n/a
Fibers analyzed on Nikon OptiPhoto 1 polarizing microscope, unless indicated as n/a under birefringence;In cases where fiber broke during transfer to glass slides, indicated as A & B; U= unconstrained; C = constrained								

APPENDIX IV
Letter of Interest
Dr. John La Scala

DEPARTMENT OF THE ARMY
US ARMY RESEARCH, DEVELOPMENT AND ENGINEERING COMMAND
ARMY RESEARCH LABORATORY
ABERDEEN PROVING GROUND MD 21005-5069

Charlene Mello
Biosciences and Technology Team
U. S. Army Natick Soldier RDECOM
Natick MA 01760-5020

January 14, 2011

Dr. Mello:

I have been working in the field of engineering polymers from renewable resources for 13 years. I have developed numerous scientific advancements, patented many of these, demonstrated such technologies on weapons platforms, and have played a significant role in commercializing these technologies. Overall, I recognize many of the challenges in developing viable engineering polymers from renewable resources, including performance, life cycle costs, and environmental benefits.

Your project, SERDP WP-1756 Identification of Important Process Variables for Fiber Spinning of Protein Nanotubes Generated from Waste Materials is one that I would like to see continue to develop. The concept of using the protein from mammalian eye lenses is highly inventive and has excellent potential. These proteins are not only renewable, but are derived from a truly abundant waste product, and thus would provide an extremely low cost starting material (and as an added benefit, could even decrease the cost of beef, fish and other food sources). Furthermore, circumventing the need for extensive sample extraction and purification prior to spinning is highly innovative. This approach should significantly reduce material cost. The properties of the resulting polymers look promising and indicate this could be a viable replacement for Nylon used for various DoD and commercial applications, including parachutes, fabrics, ropes, and in composites used in engine compartments. Clearly, more work needs to be done to achieve the level of performance required, but based on current results, this appears to be highly feasible given additional project funding. Using this material to replace Nylon has environmental benefits by replacing the toxic diacids and diamines used in this process with a renewable and water soluble polymer. Furthermore, the U.S. has a supply chain vulnerability associated with Nylon because over 95% of Nylon production takes place in China. Thus, successfully producing a polymer fiber product from mammalian eye lenses would be beneficial to the Army and commercial industry while reducing environmental impact and lowering costs.

I look forward to your progress on this project. If there is any information that I can provide to assist you in securing additional funding to further develop your material, please let me know. In the meantime, please feel free to use this as a letter of support for your project.

Sincerely,

John La Scala, Ph.D.
Acting Chief – Coatings, Corrosion, and Engineered Polymers Branch
U.S. Army Research Laboratory, WMRD, Attn: RDRL-WMM-C
Aberdeen Proving Ground, MD 21005-5069
john.lascala@us.army.mil, 410-306-0687 (ph), 410-306-0829 (FAX)